Biogeosciences, 22, 1095–1113, 2025
https://doi.org/10.5194/bg-22-1095-2025

Biogeosciences Open Access EGU

Exploring macroevolutionary links in multi-species planktonic foraminiferal Mg/Ca and $\delta^{18}O$ from 15 Ma to recent

Flavia Boscolo-Galazzo[1], David Evans[2], Elaine M. Mawbey[3], William R. Gray[4], Paul N. Pearson[3,5], and Bridget S. Wade[3]

[1]Bremen University, MARUM, Center for Marine Environmental Sciences, Bremen, Germany
[2]School of Ocean and Earth Science, University of Southampton, Southampton, UK
[3]Department of Earth Sciences, University College London, London, UK
[4]Laboratoire des Sciences du Climat et de l'Environnement (LSCE/IPSL), Université Paris-Saclay, Gif-sur-Yvette, France
[5]School of Earth and Environmental Sciences, Cardiff University, Cardiff, UK

Correspondence: Flavia Boscolo-Galazzo (flavia@uni-bremen.de)

Received: 4 June 2024 – Discussion started: 27 June 2024
Revised: 27 November 2024 – Accepted: 4 December 2024 – Published: 28 February 2025

Abstract. The ratio of the trace element Mg over Ca (Mg/Ca) and the oxygen isotopic composition ($\delta^{18}O$) of foraminiferal calcite are widely employed for reconstructing past ocean temperatures, although geochemical signals are also influenced by several other factors that vary temporally and spatially. Here, we analyse a global dataset of Mg/Ca and $\delta^{18}O$ data of 59 middle Miocene to recent species of planktonic foraminifera from a wide range of depth habitats, many of which have never been analysed before for Mg/Ca. We investigate the extent to which Mg/Ca and $\delta^{18}O$ covary through time and space and identify several sources of mismatch between the two proxies. Once the data are adjusted for long-term non-thermal factors, Mg/Ca and $\delta^{18}O$ are overall positively correlated in a way consistent with temperature being the dominant controller through both space and time and across many different species, including deep dwellers. However, we identify several species with systematic offsets in Mg/Ca values, to which multispecies calibrations should be applied with caution. We can track the appearance of such offsets through ancestor-descendent species over the last 15 Myr and propose that the emergence of these offsets may be the geochemical expression of evolutionary innovations. We find that virtually all of the Mg/Ca- and $\delta^{18}O$-derived temperatures from the commonly used genera *Globigerinoides* and *Trilobatus* are within uncertainty of each other, highlighting the utility of these species for paleoceanographic reconstructions. Our results highlight the potential of leveraging information from species lineages to improve sea surface temperature reconstruction from planktonic foraminifera over the Cenozoic.

1 Introduction

Geochemical analyses of foraminifera are commonly applied to reconstruct paleoceanographic conditions, such as marine temperatures, and therefore infer past climatic changes. In particular, the fossil tests of planktonic foraminifera (calcareous zooplankton) provide one of the most widely used paleoclimate archives. Here we focus on two of these parameters: $\delta^{18}O$ and Mg/Ca, both of which have been used widely as temperature proxies.

The oldest and possibly most widely utilized of these proxies is the ratio of oxygen isotopes in the calcite tests of these organisms, which, due to slight differences in reactivity of molecules containing the different isotopes, is temperature-dependent (Urey, 1947; see Pearson, 2012, for review). This effect has been quantified in experiments with inorganic calcite (e.g. Kim and O'Neil, 1997) and planktonic foraminifera in culture (e.g. Erez and Luz, 1983; Bemis et al., 1998). Tests of planktonic foraminifera calcifying in warmer waters are depleted in ^{18}O relative to species living in cooler waters (Emiliani, 1954). A second, more recently established paleoclimate proxy is the ratio of magnesium to calcium in test calcite (Chave, 1954; Nürnberg et al., 1996). Inorganic precipitation experiments have shown that the Mg/Ca ratio of

calcite is found to be higher at greater temperatures (Mucci, 1987). This relationship led to the in-depth exploration of Mg/Ca ratios in planktonic and benthic foraminifera and its potential application as a temperature proxy through culturing (Lea et al., 1999; von Langen et al., 2005), core top (Nürnberg, 1995; Elderfield and Gassen, 2000), and sediment trap studies (Anand et al., 2003).

As they represent two different chemical systems, the Mg/Ca and oxygen stable isotope ratios in foraminifera are often used together as independent temperature proxies. For instance, $\delta^{18}O$-derived calcification temperatures have been combined with Mg/Ca data to derive Mg/Ca temperature calibrations (e.g. Anand et al., 2003; McConnell and Thunell, 2005; Mohtadi et al., 2009). Other studies have applied these two systems together to infer the influence of environmental parameters such as seawater salinity on Mg/Ca (e.g. Mathien-Blard and Bassinot, 2009; Hönisch et al., 2013) and global ice volume (e.g. Lear et al., 2000; Katz et al., 2008). Works such as these rely on temperature being a primary driver of the two proxies for any given sample, which should be the case if both systems are impacted purely by calcification temperature. Nonetheless, there are known non-thermal effects influencing both Mg/Ca and $\delta^{18}O$. For oxygen isotope values, these include the oxygen isotopic composition of seawater ($\delta^{18}O_{sw}$) and, to a lesser degree, seawater pH or carbonate ion concentration (Spero et al., 1997; Zeebe, 1999). Seawater carbonate chemistry has also been shown to impact the Mg/Ca proxy. Culture and sediment trap studies demonstrate that surface ocean seawater pH can influence Mg/Ca in planktonic foraminifera (Lea et al., 1999; Evans et al., 2016b; Gray et al., 2018), with the sensitivity of Mg/Ca to pH appearing to vary between species (Gray and Evans, 2019). Mg/Ca values of foraminifera are also dependent on the Mg/Ca of seawater (Evans et al., 2016a), and both oxygen isotope and Mg/Ca values can be impacted by test recrystallization (Dekens et al., 2002). Mg/Ca values are susceptible to the preferential loss of Mg during dissolution and are thus influenced by the calcite saturation state of bottom waters (Regenberg et al., 2014; Tierney et al., 2019). Seawater salinity has a minor secondary effect on Mg/Ca values (Kisakürek et al., 2008; Hönisch et al., 2013), and whilst salinity has little direct effect on oxygen isotopes, a change in salinity is usually accompanied by a change in $\delta^{18}O_{sw}$ because hydrological processes such as evaporation and precipitation drive local $\delta^{18}O_{sw}$ as well as salinity (LeGrande and Schmidt, 2006). Lastly, so-called "vital effects", which lump together a wide variety of species-specific processes such as metabolism (including the process of calcification and the incorporation of metabolic products), the position within the water column and life cycle depth migration, the presence of photosymbionts, and seasonality (see summary in Schiebel and Hemleben, 2017), also add complexity to the interpretation of both the oxygen isotope and Mg/Ca proxies.

Here we use the dataset published in Boscolo-Galazzo et al. (2021) to examine covariance between Mg/Ca and $\delta^{18}O$ in planktonic foraminifera extracted from sediments across a wide range of geographic locations, time intervals, and species. The dataset is composed of $\delta^{18}O$ and Mg/Ca data measured on 59 species of planktonic foraminifera, of which 24 have never before been measured for Mg/Ca (Tables S1 and S2 in the Supplement). These data are from different ocean basins and latitudes and a range of ages between the middle Miocene ($\sim$ 15 Ma) and the Holocene. Paired Mg/Ca and $\delta^{18}O$ were measured on the same samples; hence this dataset is ideally suited to isolate potential ecological, environmental and preservational factors, which may imprint Mg/Ca or $\delta^{18}O$ or both and which are otherwise impossible to recognize in studies focusing on a limited number of species and/or a narrow study area or time interval. In particular, it provides the unique opportunity to simultaneously do the following:

1. compare coupled $\delta^{18}O$ and Mg/Ca data on a geographical and temporal scale that is broader than usual;
2. compare coupled $\delta^{18}O$ and Mg/Ca data across species of different ecologies;
3. evaluate Mg/Ca data of extinct species against those of their modern descendants;
4. test whether temperature can still be recognized as predominantly driving covariance in the dataset when spatial, temporal, and ecological variables are simultaneously in play.

2 Material and analytical methods

2.1 Material

The dataset (Boscolo-Galazzo et al., 2021) was produced from a range of globally and latitudinally distributed DSDP (Deep Sea Drilling Program), ODP (Ocean Drilling Program), and IODP (Integrated Ocean Drilling Program/International Ocean Discovery Program) sites (Fig. 1) which have a high $CaCO_3$ content and composed of calcareous nannofossils and foraminiferal pelagic oozes, with some input of siliceous plankton and clay. Sites were selected based on the best available global and temporal coverage and preservation of foraminifera. Planktonic foraminiferal preservation ranges from excellent to very good (recrystallized but lacking overgrowth and infilling; Boscolo-Galazzo et al., 2021), with the exception of Sites U1490 and U1489, where there is some overgrowth and infilling in the middle Miocene (Fayolle and Wade, 2020; Boscolo-Galazzo et al., 2021). The target ages selected for sampling were 0, 2.5, 4.5, 7.5, 10, 12.5, and 15 Ma. Biostratigraphic analysis was used to assess age using the biochronology of Wade et al. (2011) calibrated to the timescale of Lourens et al. (2004) (Table S1).

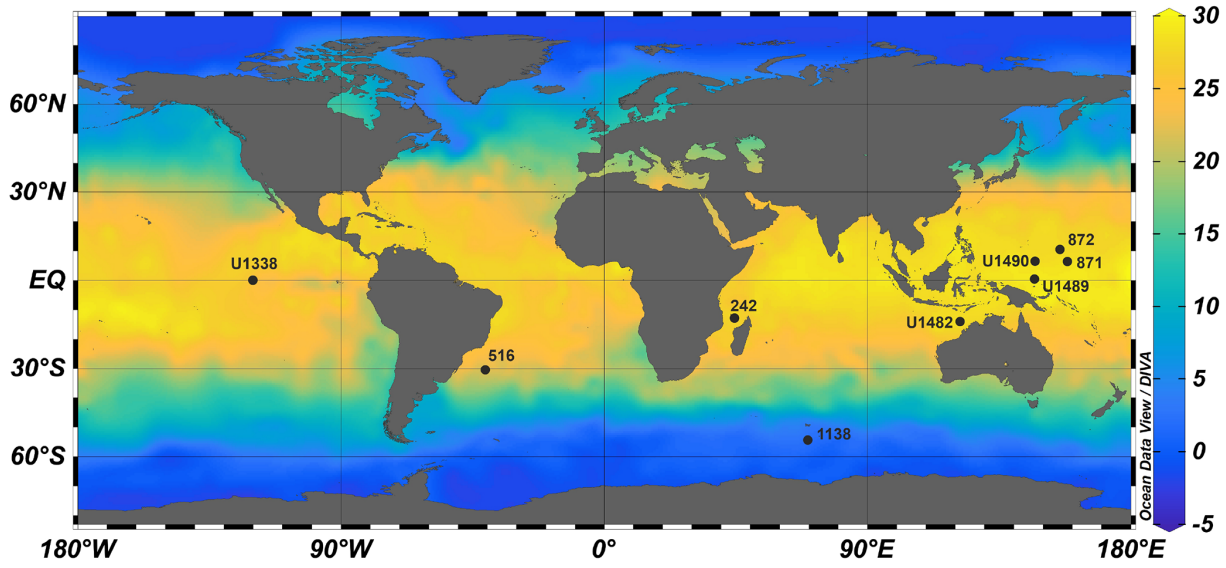

Figure 1. Site map with present-day mean annual sea surface temperatures (°C) from the World Ocean Atlas 2013 (Locarnini et al., 2013).

2.2 Planktonic foraminifera

A total of 59 species of planktonic foraminifera were analysed for Mg/Ca and $\delta^{18}O$. Planktonic foraminifera were picked from three constrained size fractions: 180–250 µm, 250–300 µm, and 300–355 µm. Planktonic foraminiferal geochemistry can change as a function of size (e.g. Birch et al., 2013), such that we used data from the size fraction 250–355 µm only, giving a total of 57 species in the dataset. For abundant species, up to 80 specimens were picked for geochemical analysis, with as many as possible picked in the case of less common species. Hence, our foraminiferal data represent an average from multiple specimens. Paleodepth habitat attributions follow Boscolo-Galazzo et al. (2021) and Boscolo-Galazzo et al. (2022). Planktonic foraminiferal taxonomy follows the concepts described in Boscolo-Galazzo et al. (2022).

2.3 Trace element and stable isotope analysis

Picked planktonic foraminifera were crushed between two glass slides to open all large chambers. When there was enough material, the crushed sample was split for stable isotope and trace element analysis. The trace element split was cleaned using a protocol to remove clays and organic matter (step A1.1–A1.3 of Barker et al., 2003). The samples did not undergo reductive cleaning due to their fragility and small sample size and because the reductive step may cause preferential removal of high Mg/Ca calcite from the test (Yu et al., 2007). Samples were dissolved in trace metal pure 0.065 M HNO_3 and then diluted with trace metal pure 0.5 M HNO_3 and analysed at Cardiff University on a Thermo Fisher Scientific Element XR ICP-MS against standards with matched calcium concentration to reduce matrix effects (Lear et al., 2002). Long-term analytical precision determined from consistency standards (CS1 and CS2) with Mg/Ca ratios of 1.24 and 7.15 mmol mol^{-1} is $\sim 0.7\,\%$ and $\sim 0.8\,\%$ (relative standard deviation). Mg/Ca was plotted against Fe/Ca and Mn/Ca to assess whether there was any relationship as a result of the presence of Fe–Mn oxyhydroxides affecting Mg/Ca, but there was no correlation between the contaminant indicators and Mg/Ca (Fig. S1).

Stable isotopes were measured on a Delta V Advantage with a GasBench II mass spectrometer at the Cardiff University stable isotope facility. Stable isotope results were calibrated to the VPDB scale using an in-house carbonate standard (Carrara marble). Analytical precision was 0.05 ‰ for $\delta^{18}O$ and 0.05 ‰ for $\delta^{13}C$.

2.4 Data analysis

Before performing the analysis, we screened the dataset for outliers and removed one anomalously high data point with a Mg/Ca value > 9 mmol mol^{-1}, which we attributed to analytical error (Table S1).

2.4.1 Formulation of theoretical relationships between Mg/Ca and $\delta^{18}O$

To test for covariation between Mg/Ca and oxygen isotope data, we regressed these data against each other and compared the observed relationship with that expected from modern calibrations. We did so to initially explore the relationship we might expect between Mg/Ca and $\delta^{18}O$ and whether this manifests in the dataset, before applying corrections for the non-thermal influences on both proxies. Given the complexity of the sample set (e.g. multiple species, ages, locations, preservation), different expected relationships between

Mg/Ca and $\delta^{18}O$ are possible, which depend on the following: (i) species-specific vital effects, (ii) non-thermal controls on Mg/Ca (salinity, pH, Mg/Ca_{sw}), and (iii) non-thermal controls on $\delta^{18}O$ (pH/$[CO_3^{2-}]$), $\delta^{18}O_{sw}$, as well as how these factors change through time. To account for this, we calculated a number of possible expected theoretical relationships to give a sense of how much of the scatter in the raw data is likely to be explicable by these factors and inform our following data analysis accordingly. We stress that this exercise was conducted as an initial exploration of the dataset; no single relationship will be able to explain the dataset because it is influenced by multiple, often interlinked, variables.

Expected theoretical relationships were calculated starting with modern laboratory culture calibrations, onto which the key non-thermal long-term and spatial controls on these proxies were sequentially added to demonstrate how much each of these is expected to shift the slope of the expected Mg/Ca–$\delta^{18}O$ relationship (Fig. 2a). Specifically, we did the following:

i. combined the Mg/Ca temperature calibrations for *Globigerinoides ruber* and *Trilobatus sacculifer* of Gray and Evans (2019) with the $\delta^{18}O$–temperature equation of Erez and Luz (1983);

ii. added the impact of a 0.15 unit whole-ocean pH change (approximating the magnitude of the Neogene whole-ocean change, e.g. Rae et al., 2021) using the pH–Mg/Ca slope for *G. ruber* as an example (note that this is only applicable to species that show a pH sensitivity) (Evans et al., 2016b);

iii. included the expected control of temperature on pH via the T-dependent dissociation of water (K_W), i.e. temperature-driven pH changes within a given time interval independent of whole-ocean pH shifts (Gray et al., 2018);

iv. showed the impact of Mg/Ca_{sw} half of the modern ratio (Evans et al., 2016a);

v. included the effect of pH or $[CO_3^{2-}]$ on $\delta^{18}O$ (Spero et al., 1997; Zeebe, 1999) given the covariance of temperature and pH described in point (iii) above using the multispecies average slope of Gaskell and Hull (2023); and, finally,

vi. explored the likely impact of the covariance of $\delta^{18}O_{sw}$ and temperature that is characteristic of the modern ocean and arises from the broad coupling of the hydrological cycle with surface temperatures.

This latter influence was calculated by combining sea surface temperature (SST) data from the 2013 World Ocean Atlas (Locarnini et al., 2013) and $\delta^{18}O_{sw}$ from LeGrande and Schmidt (2006), taking all surface ocean data except those from polar meltwater regions, which demonstrates that, on average, in the modern ocean $\delta^{18}O_{sw}$ increases by 0.0425 ‰ per degree (Celsius) of SST increase.

Each of these factors was applied additively such that factor (iv) listed above (Mg/Ca_{sw}) in Fig. 2 includes factors (i) through (iii). The sum of the influence of these factors on the theoretical $\delta^{18}O$–Mg/Ca relationship is represented by the thick blue line in Fig. 2a and the black line in Figs. 2b, 3, 5, 6, and 7, which has a slope of −2.08 in $\delta^{18}O$–ln(Mg/Ca) space.

The magnitude of some of these potential non-thermal controls on the two proxies over the time interval studied here is reasonably well constrained. Specifically, the long-term whole-ocean pH and Mg/Ca_{sw} changes are sufficiently well known (Rae et al., 2021; Zhou et al., 2021; Brennan et al., 2013) that they can be "subtracted" out of the raw proxy values, given that they are likely to apply to all or most species in the dataset. As such, we next explored the degree to which the Mg/Ca–$\delta^{18}O$ covariation improves once long-term whole-ocean pH and Mg/Ca_{sw} changes are removed. To avoid (possibly incorrect) a priori assumptions regarding, for example, which Mg/Ca–temperature calibration should be applied to each species in the dataset and the degree to which surface ocean $\delta^{18}O_{sw}$ has varied at the study sites, we initially kept the Mg/Ca and $\delta^{18}O$ comparison in raw proxy space and did the following: (1) converted the raw Mg/Ca values to temperature using the multispecies Mg/Ca–temperature calibration from Gray and Evans (2019), together with our best estimate of pH and Mg/Ca_{sw} (as described below (Sect. 2.4.2)), and (2) converted the temperatures back into Mg/Ca using the same calibration but modern seawater Mg/Ca and pH. Conceptually, this is equivalent to correcting the raw proxy values for these nonthermal controls. In addition, we subtracted out the long-term whole-ocean change in $\delta^{18}O_{sw}$ related to continental ice growth using the sea level curve of Rohling et al. (2022) and a sea level–$\delta^{18}O_{sw}$ scaling factor of 1 ‰ per 67 m. This results in a raw proxy dataset in which the aforementioned long-term non-thermal factors are no longer present and which can be used to evaluate the occurrence of residual scatter independent of the long-term non-thermal controls on Mg/Ca and $\delta^{18}O$ (Fig. 2b).

2.4.2 Transformation of proxy values into paleotemperature

Measured foraminifera Mg/Ca was transformed into paleotemperature using the MgCaRB tool (Gray and Evans, 2019; https://github.com/dbjevans/MgCaRB/releases/tag/v1.3, last access: 11 February 2025 (MATLAB); https://doi.org/10.5281/zenodo.14056982) which takes the following into account:

– *Salinity*. Although this has a minor effect on Mg/Ca (Hönisch et al., 2013), whole-ocean changes are nonetheless accounted for using a salinity reconstruc-

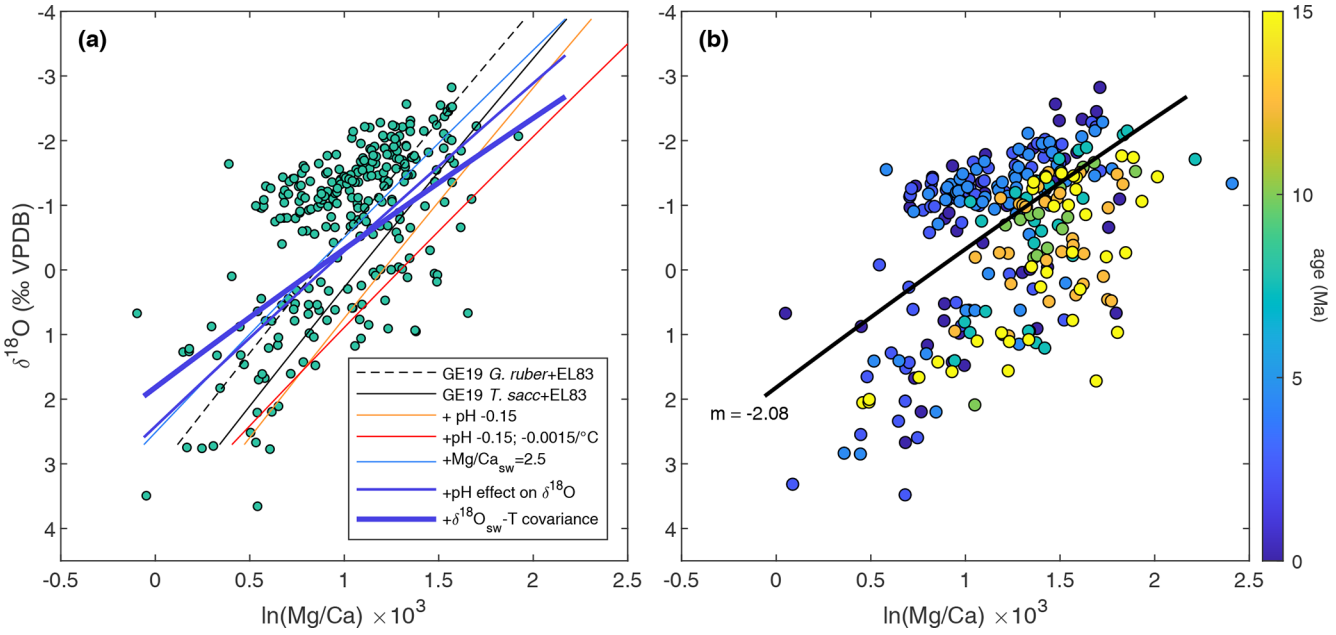

Figure 2. Raw δ^{18}O plotted against Mg/Ca for all samples presented here. **(a)** Several possible expected Mg/Ca–δ^{18}O slopes are shown for comparison, including the slope for *G. ruber* and *T. sacculifer* (at constant pH) in the modern ocean (solid and dashed black lines respectively). The additive impact of nonthermal controls is then explored using the *G. ruber* calibration as an example, specifically **(a)** the impact of a whole-ocean pH shift of 0.15 units (orange line), accounting for the covariation of pH and temperature (driven by the temperature-dependent dissociation of water, red line), seawater Mg/Ca half of the present day value (thin blue line), the theoretical impact of pH on δ^{18}O (blue line), and the covariance of temperature and $\delta^{18}O_{sw}$ in the modern ocean (thick blue line). We stress that the magnitude of the pH, Mg/Ca$_{sw}$, and $\delta^{18}O_{sw}$ changes applied to these theoretical lines was chosen to illustrate the sensitivity of the two proxies to these factors and does not necessarily represent the degree to which these factors differed in any specific time interval compared to today. The length of each line depicts the expected Mg/Ca and δ^{18}O change across the same temperature range in each case (5–35 °C). All calculations assume $\delta^{18}O_{sw} = 0‰$. **(b)** As in panel **(a)**, except with the long-term whole-ocean changes in pH, Mg/Ca$_{sw}$, and $\delta^{18}O_{sw}$ subtracted from the raw proxy values (see text, using the multispecies calibration of Gray and Evans, 2019, in the case of the Mg/Ca corrections), i.e. accounting for the impact of these non-thermal Mg/Ca and δ^{18}O controls. Sample age is shown as a function of colour. Note that the black line is not a regression but rather shows one possible theoretical Mg/Ca–δ^{18}O relationship and is identical to the thick blue line from panel **(a)** including the combined effect of all factors explored there. The slope of this theoretical relationship is −2.08, which provides an approximate expected slope of Miocene–recent Mg/Ca versus δ^{18}O, although we note that no real-world dataset will conform exactly to this as pH, Mg/Ca$_{sw}$, and $\delta^{18}O_{sw}$ have not (perfectly) covaried through time.

tion derived from scaling the δ^{18}O benthic stack (Westerhold et al., 2020) to the sea level record of Spratt and Lisiecki (2016) between 0.8 and 8 Ma, of Rohling et al. (2022) between 8 and 40 Ma, and assuming an ice-free world before this time. We applied the multispecies salinity sensitivity of Gray and Evans (2019) to all species (3.6 % per salinity unit).

– *pH*. Long-term whole-ocean changes were derived from a smoothing spline fit to the boron-isotope-derived pH data compiled by Rae et al. (2021). We applied species-specific pH–Mg/Ca sensitivities of Gray and Evans (2019) where available for a given species/lineage (discussed in more detail below) and used the multispecies sensitivity in all other cases.

– Mg/Ca$_{sw}$. This was derived by combining the [Ca^{2+}_{sw}] record of Zhou et al. (2021) with a smoothing spline fit to the fluid inclusion [Mg^{2+}_{sw}] data given in Brennan et al. (2013). Raw Mg/Ca values were adjusted using the equation $Mg/Ca_{corrected} = Mg/Ca_{raw} \times Mg/Ca^{H}_{sw}/5.2^{H}$, where $H = 0.64$ based on a data compilation of three foraminifera species and inorganic calcite (Holland et al., 2020; Evans et al., 2015, 2016b; Mucci and Morse, 1983).

We initially applied a multispecies equation because the dataset includes a mix of extant and extinct species, some of which have never been measured for trace elements before (Table S2) or lack an extant/well-calibrated modern relative. Specifically, we used the multispecies Mg/Ca–temperature equation of Gray and Evans (2019) and applied the multispecies pH, salinity, and temperature sensitivities, together with the *Globigerinoides ruber* pre-exponential coefficient

(given a Mg/Ca–T relationship of the form Mg/Ca = BeAT in its simplest form) as most of the species for which high-quality data exist are known to be characterized by a Mg/Ca–pH sensitivity (Lea et al., 1999; Kisakürek et al., 2008; Evans et al., 2016b).

We subsequently applied species-specific calibrations to selected lineages to explore the degree to which scatter in the dataset can be accounted for by taking into account phylogenetic relationships among ancestor-descendent species. Specifically, the *Trilobatus sacculifer* calibration was applied to the *Trilobatus trilobus–Trilobatus sacculifer* lineage, and the *Orbulina universa* calibration was applied to the *Praeorbulina–Orbulina* lineage, both from laboratory culture studies following Gray and Evans (2019). To *Neogloboquadrina* and its descendent lineage *Pulleniatina* we applied a *Neogloboquadrina pachyderma* calibration with the sensitivities (and their uncertainties) of Tierney et al. (2019) (implemented with a re-fit to the dataset following the MgCaRB approach; see Fig. S1). We then evaluate the improvement relative to the multispecies calibration in samples spanning the middle Miocene to modern. The attribution of phylogenetic relationships follows Aze et al. (2011), Spezzaferri et al. (2018), Leckie et al. (2018), and Fabbrini et al. (2021). All uncertainties were fully propagated via Monte Carlo simulation, including those related to analysis; calibration coefficients (the coefficients that relate Mg/Ca to temperature, pH, and salinity); and the 95 % confidence intervals on the salinity, pH, and Mg/Ca_{sw} reconstructions. Specifically, 10^4 random draws of each of these values within their respective uncertainty bounds were used to generate the reported values and 95 % CI (percentiles 2.5, 50, and 97.5 of the resulting dataset). The relative contributions of the various nonthermal factors impacting Mg/Ca-derived temperature are shown in Fig. S2.

The conversion of $\delta^{18}O$ to paleotemperature followed Gaskell and Hull (2023) using the bayfox calibration (Malevich et al., 2019) and the global and local $\delta^{18}O_{sw}$ of Rohling et al. (2022) and Gaskell and Hull (2023) respectively. The calculation was performed twice, both with and without a pH/$[CO_3^{2-}]$ effect on $\delta^{18}O$ (the former using the mean planktonic foraminiferal slope of Gaskell and Hull (2023), and the $[CO_3^{2-}]$ record of Zeebe and Tyrrell, 2019). We also explored the impact of using a different sea level/deep-ocean temperature reconstruction (Miller et al., 2020) on our results, described in the Results Section and shown in Fig. S3.

When evaluating the paleotemperature reconstructions, we define whether or not the two proxy systems agree within uncertainty by determining if the root sum of squares of the two uncertainties is smaller than the temperature difference between the two proxies. We then proceed to identify possible drivers for the data deviating from the expected Mg/Ca and $\delta^{18}O$ relationship by evaluating the age of the sample, regional changes in $\delta^{18}O_{sw}$, depth ecology, and possible species-specific offsets.

We note that all of the above corrections assume surface ocean conditions, while the dataset contains a number of species that calcify at depth (Boscolo-Galazzo et al., 2021). Given the uncertainties surrounding past changes in vertical pH and $\delta^{18}O_{sw}$ profiles, we do not attempt to account for this in our data analysis but note that this consideration should be borne in mind when interpreting data from deep-dwelling species.

3 Results

Our basic expectation is that higher Mg/Ca should relate to more negative $\delta^{18}O$ values for warmer temperatures and vice versa for colder temperatures. Despite the large number of variables included, the dataset as a whole shows a positive correlation (Fig. 2a; $R^2 = 0.37$, RMSE = 1.01, $p \ll 0.01$) between $\delta^{18}O$ and ln(Mg/Ca). Hence, the $\delta^{18}O$–Mg/Ca covariance can be considered a robust feature over the past 15 Myr for the majority of the species analysed and across the study sites. Nonetheless, there is a high degree of scatter in these data, which suggests that the temperature signal which should lead Mg/Ca and $\delta^{18}O$ data to change consistently in opposite directions is affected by other factors. Our exercise of generating theoretical Mg/Ca–$\delta^{18}O$ relationships (Fig. 2), exploring how the relationship between the two proxies might change through space and time, provides a qualitative indication as to whether the scatter can be attributed to long-term non-thermal factors generally corrected for when using the $\delta^{18}O$ and Mg/Ca proxies. The substantial differences between these expected relationships suggests that this is likely to be the case (Fig. 2a). In particular, Fig. 2a suggests that both a pH effect and Mg/Ca_{sw} changes through time may explain a substantial degree of the variability observed in the dataset compared to the modern relationships (compare the coloured and black lines; see also Fig. S2). Nonetheless, accounting for these long-term biases alone in the raw dataset does not remove all of the scatter (Fig. 2b), suggesting the importance of additional factors, such as vital effects and regional variations in $\delta^{18}O_{sw}$. Data converted into temperature, along with 95 % confidence intervals, are shown in Fig. 3. In this plot 62 % of data points fall within uncertainty, confirming that a high degree of variability in the raw data can be effectively explained and accounted for by correcting for the known spatially and temporally varying non-thermal effects influencing both proxies.

Using the deep-ocean temperature and sea level records of Miller et al. (2020) rather than Rohling et al. (2022) (Fig. S3) would shift our $\delta^{18}O$ temperature reconstructions of +0.5 to 3.3 °C depending on sample age, with the samples from the 7.5 Ma time slice being most affected. Whilst the choice to correct for global $\delta^{18}O_{sw}$ exerts a significant control on $\delta^{18}O$-derived temperatures, it has a minor impact on both our long-term dataset overall (compare Fig. 3 with Fig. S3) and

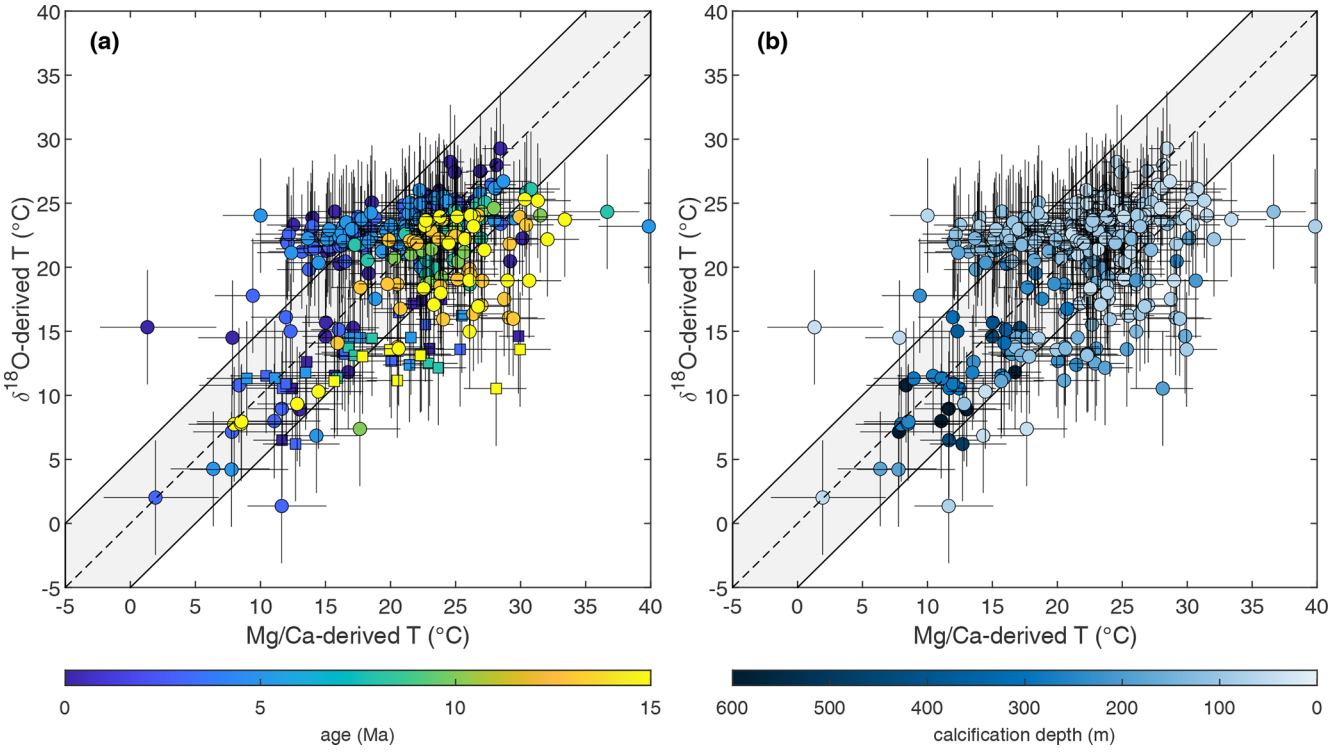

Figure 3. δ^{18}O- versus Mg/Ca-derived paleotemperatures plotted as a function of age **(a)** and calcification depth **(b)**, accounting for the impact of whole-ocean and regional changes in $\delta^{18}O_{sw}$ following Gaskell et al. (2022) using the bayfox δ^{18}O–temperature calibration (Malevich et al., 2019), whole-ocean changes in Mg/Ca_{sw} and pH on Mg/Ca using MgCaRB (Gray and Evans, 2019), and including a pH correction on δ^{18}O using the mean planktonic foraminifera slope (Gaskell and Hull, 2023). The grey envelopes in **(a)** and **(b)** are fully propagated uncertainties in both proxies incorporating analysis, calibration, pH, Mg/Ca_{sw}, and $\delta^{18}O_{sw}$/salinity, while the dotted black lines are identical to the thick blue and black lines in Fig. 2a and b (see text for details). Site 516 data are shown with square symbols in panel **(a)**.

the proportion of proxy data within combined uncertainty, from 62 % to 64 %.

We find that deep-dwelling and surface-dwelling species fall within uncertainty in terms of the broad degree of agreement between Mg/Ca- and δ^{18}O-derived temperatures; hence different depth-habitat ecologies or calcification environments do not represent a systematic source of offset per se (Fig. 3b). Indeed, all the species displaying a temperature offset between the two proxies are surface dwellers (0–200 m depth, Boscolo-Galazzo et al., 2022), with deep dwellers characterized by inter-proxy agreement in almost all cases (Fig. 3b). Additional explanations are required for those temperature reconstructions that, all non-thermal and spatial controls included, still plot outside their propagated error uncertainty. Data points outside the combined proxy uncertainties either display > 5 °C warmer (colder) δ^{18}O (Mg/Ca) temperatures (upper-left area of the plot) or > 5 °C warmer (colder) Mg/Ca (δ^{18}O) temperatures (bottom-right area of the plot) (Fig. 3).

Figure 3a clearly shows that the large majority of the outliers in the upper-left part of the plot (warmer δ^{18}O temperatures or cooler Mg/Ca temperatures) are species of late Miocene to modern age, while the outliers in the bottom-right part of the plot (warmer Mg/Ca temperatures) are mostly older species of middle Miocene age or from mid-latitude Site 516 (squares in Fig. 3a). We suggest and discuss possible main sources for these offsets between Mg/Ca and δ^{18}O temperatures in detail below.

4 Discussion

4.1 Diagenesis

Diagenesis is known to alter the test chemistry of foraminifera in three main ways: partial dissolution, overgrowth, and recrystallization (Edgar et al., 2015). The trace element and isotopic composition of tests react differently to these diagenetic processes. The trace element composition of foraminiferal calcite may be susceptible to partial dissolution because it is inhomogeneous (Fehrenbacher and Martin, 2014), which decreases trace element ratios in species with high- and low-Mg regions (Dekens et al., 2002; Edgar et al., 2015; Rongstad et al., 2017), resulting in lower temperature reconstructions. Overgrowth and recrystallization have been shown to add both low-Mg and high-Mg diagenetic calcite, potentially impacting the original signal in opposite direc-

tions (Branson et al., 2015), although Mg/Ca is relatively robust to this type of diagenesis, at least in certain circumstances (Staudigel et al., 2022). The oxygen isotopic composition of planktonic foraminiferal tests is well known to be very sensitive to overgrowth and recrystallization (e.g. Sexton et al., 2006), whereby the addition of diagenetic calcite, or the replacement of the original calcite with diagenetic calcite precipitated at the seafloor, can significantly alter the original isotopic signal, shifting it to more positive values (Pearson, 2012; Edgar et al., 2015).

The Boscolo-Galazzo et al. (2021) dataset spans 15 Myr and includes sites with different average preservation of foraminiferal tests and oceanographic settings. When these data are regressed against each other (Fig. 2b), we find a total of 26 data points characterized by oxygen isotope values more positive than expected from their Mg/Ca values (Fig. 2b; Table S1), resulting in $\delta^{18}O$ temperatures $> 5\,°C$ colder than Mg/Ca temperatures (outside the error envelope) (Fig. 3; Table S1). Of these data points, 21 were from the older time slices (12.5 Ma and 15 Ma), 1 from the 7.5 Ma time slice and 4 from the core top of Site U1338 (Table S1).

As the majority of these data points were characterized by Mg/Ca values of ~ 1.5–$2\ln(Mg/Ca)$ (Fig. 2b), thus yielding more reasonable Mg/Ca than $\delta^{18}O$ temperatures for these sites/time intervals (Table S1), the observed offset is most likely best attributed to diagenetic overgrowth/recrystallization, shifting oxygen isotopes towards more positive values without affecting Mg/Ca to the same extent. A recent study compared typical Mg/Ca–$\delta^{18}O$ from recrystallized planktonic foraminifera with chemical diffusive models simulating early diagenetic processes in calcite (Staudigel et al., 2022). According to that study, in a closed system, the bulk $\delta^{18}O$ value will be altered faster than the Mg/Ca, regardless of what partitioning coefficient is used for Mg, leading to a progressive shift to more positive $\delta^{18}O$ values leaving Mg/Ca virtually unchanged (Staudigel et al., 2022).

Data points characterized by $\delta^{18}O$ overprinted by overgrowth/recrystallization were distributed across most of the study sites (except for Sites 871/872), but they were more common at Site U1490 and U1489 (15/26) which are characterized by inferior preservation compared to the others (Boscolo-Galazzo et al., 2021). The core top samples at Site U1338 show clear signs of dissolution with highly fragmented tests. These data points presented the lowest Mg/Ca values in the dataset (1.68 and 0.91 $mmol\,mol^{-1}$), with temperatures from Mg/Ca lower than from $\delta^{18}O$. This suggests that partial dissolution and recrystallization affected both Mg/Ca and $\delta^{18}O$ in this sample but Mg/Ca more so.

Overall, our scrutiny for diagenesis of the Boscolo-Galazzo et al. (2021) dataset is consistent with previous studies suggesting that $\delta^{18}O$ values are more easily affected by recrystallization than Mg/Ca (Sexton et al., 2006; Staudigel et al., 2022; John et al., 2023), similar to other trace element systems (Edgar et al., 2015).

Based on the considerations above we excluded the affected 26 data points from the subsequent analysis as being characterized by a stronger diagenetic overprint than the rest of the dataset (Table S1). Removing the affected data points in some but not all the cases equated to removing a whole sample (Table S1). This is because of variable diagenetically offset $\delta^{18}O$ values from different species in a sample, as observed elsewhere (Sexton et al., 2006; Edgar et al., 2015). The approach used here to reconstruct $\delta^{18}O$ temperature shows that for the rest of the study dataset a diagenetic offset would be comprised within the propagated error envelope ($\sim$ 2–2.5 °C) (Fig. 3) and comparable or not distinguishable from an offset deriving from poorly constrained $\delta^{18}O_{sw}$.

4.2 Regional-scale spatial heterogeneity in seawater chemistry

Once converted into temperatures the dataset shows an overall good Mg/Ca–$\delta^{18}O$ agreement, consistent with temperature being a dominant controller of both proxies through time and across the broad geographical area investigated (Fig. 3). This suggests that, by and large, the seawater corrections applied for the local and global changes in ocean chemistry are adequate, although for one site this may not hold true. Site 516 is a mid-latitude site (south-west Atlantic, 30° S) characterized by a modern sea surface temperature around 20 °C (Fig. 1); most of these data points from this site have very positive $\delta^{18}O$ values associated with high Mg/Ca (Fig. 2b; Table S1). Once converted, this results in $\delta^{18}O$ temperatures that are too cold (12–17 °C) compared to both modern (given long-term warming since the Miocene is not expected at any of these sites) and the equivalent Mg/Ca temperatures from the same samples, which are around 21–25 °C (Fig. 3a; Table S1). We do not attribute this mismatch to diagenesis for a number of reasons. First, Site 516 is characterized by a very good test preservation, much better than at Site U1489 and U1490 for which diagenesis extensively affects the middle Miocene samples; second, this mismatch is observed in the entire dataset through samples spanning the middle Miocene to modern; and third, the mismatch is observed for surface-dwelling species only, with deep dwellers characterized by $\delta^{18}O$–Mg/Ca in good agreement. Site 516 is situated in an area of complex surface hydrography, as it sits at the confluence between the warm Brazil western boundary current and the cold Falkland (Malvinas) Current spinning off from the Antarctic Circumpolar Current (e.g. Jonkers et al., 2021). Compared to the subtropical gyres, where many of the study samples come from, a large degree of spatial variability of surface water physical–chemical properties can be expected on a seasonal and multiannual scale. As such, we suggest that the mismatch between $\delta^{18}O$ and Mg/Ca observed in surface-dwelling species at Site 516 may result from changeable surface water properties from the mixing of two very different water masses creating deviations in pH, salinity, and $\delta^{18}O_{sw}$ beyond those that are typical in stratified open ocean environ-

ments and that are difficult to correct for. Sites with a changeable hydrography, such as Site 516, may hence not be ideal for the application of geochemical proxies affected by seawater chemistry, unless changes in seawater chemistry at the site can be reconstructed directly.

4.3 Species-specific offsets

The third and largest source of mismatch that we consider is the occurrence of species-specific offsets, particularly in Mg/Ca given that, in general, the relative degree of inter-species Mg/Ca variability is greater than for oxygen isotopes. For example, the range of inter-species δ^{18}O offsets is around 1 ‰ (< 4 °C), whereas there may be more than a factor of 2 difference in Mg/Ca between species for a given temperature (e.g. compare Pearson, 2012; Gray and Evans, 2019; Regenberg et al., 2009; Däeron and Gray, 2023). When regressing these data against each other, we find several species characterized by systematically offset Mg/Ca values (e.g. Fig. 2b; Table S1) leading to proxy–proxy disagreement (Fig. 3; Table S1). The occurrence of such offset Mg/Ca values is not evenly distributed across species but is shared among related species in both spinose and non-spinose groups (Figs. 4 and 5; Table S1). Specifically, the spinose species *Orbulina universa* (2 out of 5 specimens, 2/5), *O. suturalis* (3/6), and *Praeorbulina glomerosa* (1/1) present high Mg/Ca ratios compared to their δ^{18}O values and Mg/Ca of other species (Fig. 5e). We also find that *Globigerinella siphonifera* (6/7), *G. calida* (1/1), *G. praesiphonifera* (3/4), and *Globigerina bulloides* (5/6) have offset Mg/Ca–δ^{18}O values, largely being characterized by higher-than-expected Mg/Ca, although three *G. siphonifera* data points show lower Mg/Ca (Figs. 4 and 5k; Table S1). Among non-spinose species, *Neogloboquadrina humerosa* (11 out of 12 specimens, 11/12), *N. acostaensis* (3/3), *Pulleniatina obliquiloculata* (5/6), *P. praecursor* (3/5), *P. primalis* (4/6), *Sphaeroidinella dehiscens* (4/4), and *Sphaeroidinellopsis paenedehiscens* (5/10) display Mg/Ca values lower than expected for their oxygen isotope composition (Figs. 4 and 5g, i; Table S1). For the first time, these results highlight the occurrence of similarly offset Mg/Ca values for ancestor-descendent species belonging to the same lineage as well as for whole new lineages (Figs. 4 and 5).

Divergent Mg/Ca values for *G. siphonifera* and *O. universa* have previously been reported (Opdyke and Pearson, 1995; Anand et al., 2003; Friedrich et al., 2012). In the case of *O. universa*, the offset may be related to pH change in the foraminiferal microenvironment due to symbiont photosynthetic activity (Eggins et al., 2004) or changes in seawater pH, with Mg/Ca of the test increasing by as much as $6\% \pm 3\%$ for each 0.1 unit decrease in pH (Lea et al., 1999; Russell et al., 2004). pH-related vital effects are reported for other spinose species of planktonic foraminifera such as *Globigerina bulloides* (Lea et al., 1999; Davis et al., 2017), which is related to the genus *Globigerinella* (Fig. 4).

Among the neogloboquadrinids, *N. acostaensis* and its descendant *N. humerosa* have the most clearly expressed offset with low Mg/Ca values in the study dataset. In contrast, *Neogloboquadrina pachyderma* and *N. incompta* are not offset in the study dataset, perhaps simply because of the limited number of data (one data point each). More broadly, a Mg/Ca offset compared to other species has been reported in the literature (Davis et al., 2017). *Neogloboquadrina dutertrei*, *N. incompta*, *N. pachyderma*, and *Pulleniatina obliquiloculata* have been shown to be characterized by much lower trace element concentrations (Mg–Ba–Zn/Ca) in the adult portions of their shells (crust and cortex), so that a greater amount of adult versus early ontogenetic calcite leads to low trace element values in bulk shell analysis (Jonkers et al., 2012; Davis et al., 2017; Fritz-Endres and Fehrenbacher, 2021). The low Mg/Ca of crust and cortex has been found to be independent of ambient temperature in cultured *Neogloboquadrina* (Davis et al., 2017). It is found in specimens collected both in surface waters and at depth (Jonkers et al., 2021), indicating that the low Mg/Ca is not acquired due to calcification in deeper, colder waters of the crust/cortex portion of the shell, although a greater incidence of crusts is reported for colder waters (Jonkers et al., 2021). *Neogloboquadrina*, *Pulleniatina*, and *Sphaeroidinella/Sphaeroidinellopsis* are all characterized by a thick crust or cortex, suggesting their Mg/Ca is biased by low Mg adult calcite being quantitatively predominant, which is further corroborated by their Mg/Ca being unrelated to temperature in our data and consistently falling outside of the δ^{18}O-derived temperatures, even accounting for the combined uncertainty of the two proxies (Fig. 5g–h and i–j).

The majority of the data points from the offset spinose and non-spinose species result in temperature differences between the two proxies greater than 5 °C when using the multi-species calibration from Gray and Evans (2019) as described in Sect. 2.4.2, hence outside the calculated error envelope when taking all the non-thermal factors discussed above into account (Fig. 5). A similar temperature offset is not apparent for other lineages such *Trilobatus trilobus–Trilobatus sacculifer* and *Globigerinoides subquadratus–G. ruber*, to which the same treatment to the offset spinose and non-spinose species was applied (Sect. 2.4.2, Fig. 5a–d). Hence, we attribute the offset temperatures to the atypical Mg/Ca signatures described above in the affected species, in turn resulting from biology-/ecology-dependent vital effects shared within a lineage and between related lineages (Figs. 4 and 5).

When a species-specific calibration for *Neogloboquadrina pachyderma* is applied to descendent species/lineages and sister taxa (Fig. 6) the offset is successfully corrected for all the *Neogloboquadrina* and *Pulleniatina* species which effectively no longer produce offset temperatures (Fig. 6). In contrast, we only observe a minor improvement when applying the *Orbulina universa* calibration to the *Praeorbulina–Orbulina* lineage, with most temperature data points remaining offset (Fig. 6). This may imply that the *O. universa* lab-

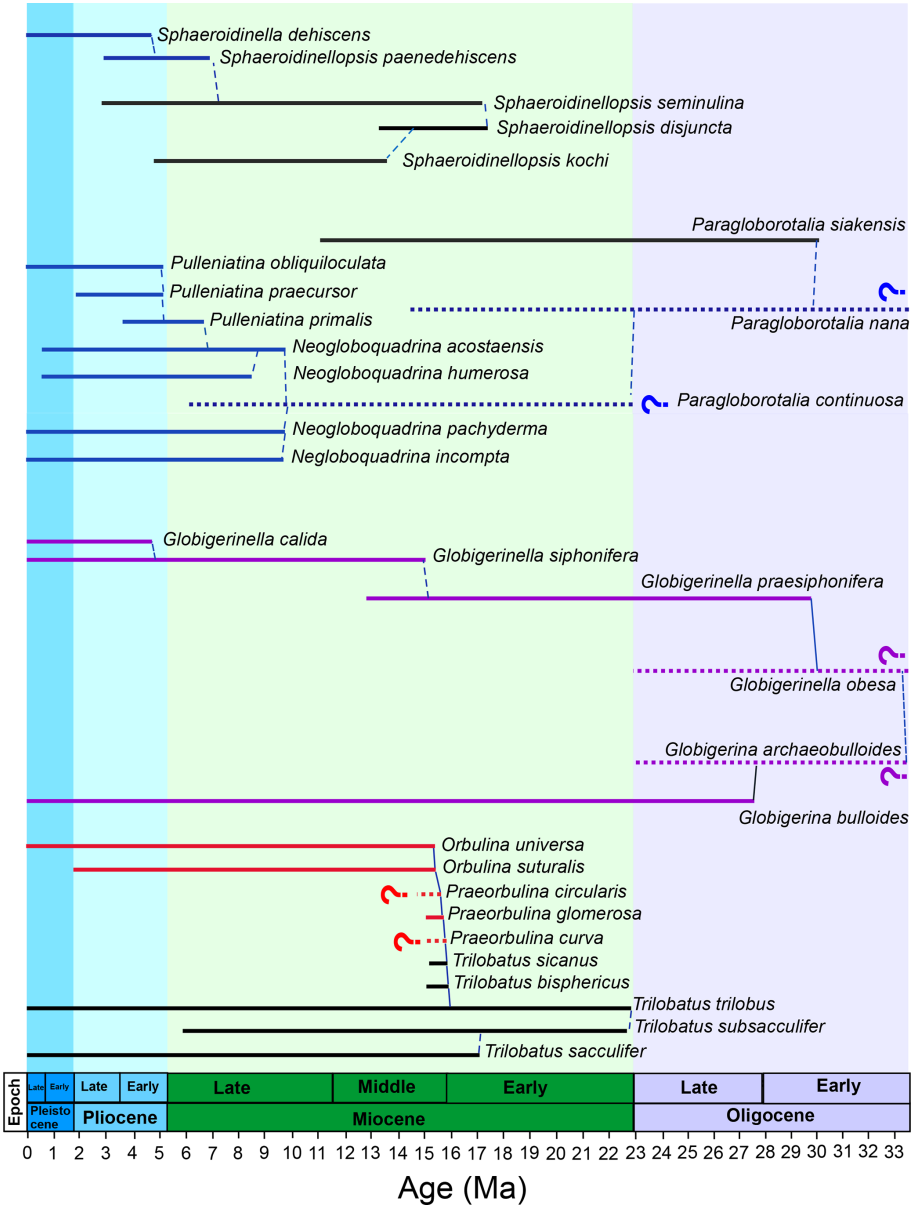

Figure 4. Phylogenetic relationships of offset spinose and non-spinose species. Shown here are the species discussed in the text and their most closely related species and ancestors. Coloured lines indicate species offset in Mg/Ca in the study dataset relative to a multispecies calibration approach, and black lines indicate non-offset species. Red lines indicate offset species with higher Mg/Ca, blue lines offset species with lower Mg/Ca, and purple lines species displaying both types of offsets. Question marks indicate the lack of Mg/Ca data for a given species in the dataset presented here. Phylogeny after Aze et al. (2011), Spezzaferri et al. (2018), Leckie et al. (2018), and Fabbrini et al. (2021). The phylogenetic chart was generated using Mikrotax (Huber et al., 2016; http://www.mikrotax.org/pforams, last access: 4 June 2024). Ages are from Lourens et al. (2004) for the Neogene and Pälike et al. (2006) for the Oligocene.

oratory calibrations require revision for application to fossil samples. No large difference is observed when applying the *Trilobatus sacculifer* calibration to ancestor-descendent species in the genus *Trilobatus* (Figs. 5–7) although we recommend doing so, given that no Mg/Ca–pH effect is known for this genus, in contrast to (e.g.) *G. ruber*.

Overall, this exercise demonstrates that the majority of data points characterized by proxy–proxy disagreement (Fig. 3) are from the lineages *Praeorbulina–Orbulina*, *Globigerina–Globigerinella*, *Neogloboquadrina–Pulleniatina*, and *Sphaeroidinellopsis–Sphaeroidinella* (Fig. 5). We find that using a "nearest descendant" approach in the choice of temperature calibration improves the agreement between $\delta^{18}O$ and Mg/Ca temperatures for the neogloboquadrinids and pulleniatinids (Fig. 6). At the same time, it enables us to identify "problematic" species and

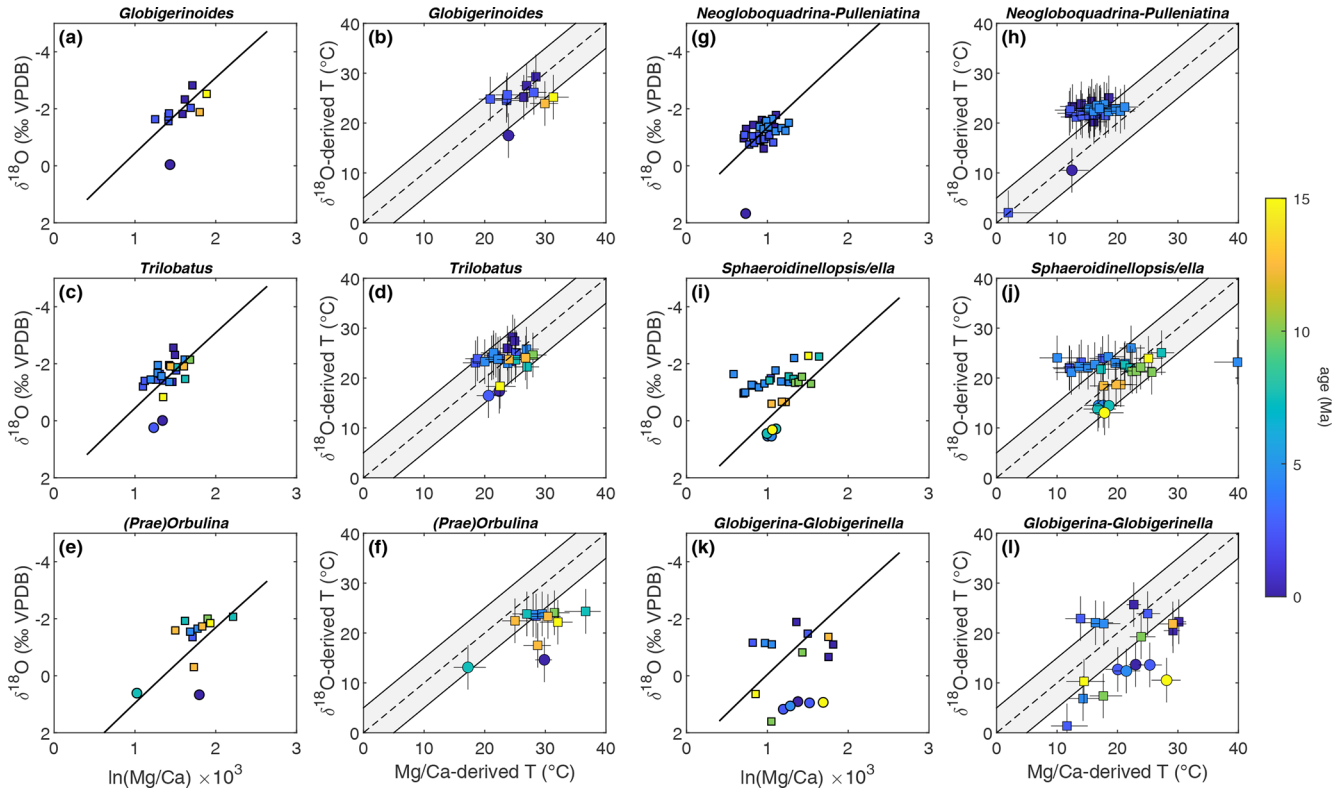

Figure 5. δ^{18}O versus Mg/Ca and proxy-derived paleotemperature estimates for the ancestor-descendent species *Globigerinoides subquadratus–G. ruber* **(a, b)**; *Trilobatus trilobus–T. sacculifer* **(c, d)**; *Praeorbulina glomerosa–Orbulina suturalis–O. universa* **(e, f)**; *Neogloboquadrina acostaensis–N. humerosa*, *N. pachyderma–N. incompta*, and *N. acostaensis–Pulleniatina primalis–P. praecursor–P. finalis* **(g, h)**; *Sphaeroidinellopsis seminulina–S. paenedehiscens–Sphaeroidinella dehiscens* and *S. seminulina–S. kochi* **(i, j)**; and *Globigerinella praesiphonifera–G. siphonifera–G. calida* and *Globigerina bulloides* **(k, l)**. Species are defined as offset relative to a multispecies calibration approach when their reconstructed temperature plots outside the grey error envelope (see text for details). Circles indicate data points from Site 516. Raw proxy values are given with the long-term non-thermal controls on Mg/Ca subtracted out (as in Fig. 2), as well as an estimate of paleotemperature (as in Fig. 3). The continuous and dotted black lines depict one possible estimate of the expected slope between δ^{18}O and Mg/Ca (the thick blue and black lines from Fig. 2), adjusted to approximately match the location of these data by shifting them in the direction of δ^{18}O. Data points which are considered strongly affected by diagenesis are not included in this plot. Note that one data point in panel **(g)** falls outside of the plot area.

lineages which require further investigations before being used for temperature reconstructions (Fig. 6). Once all the potential sources of offset described above are taken into account, the species-specific calibration for *Neogloboquadrina* is applied, and data points which are still offset are removed from the dataset, the agreement between the two proxies increased from 62 % to 91 % of data points falling within the combined uncertainties of the proxies (Fig. 7).

4.4 Planktonic foraminiferal Mg/Ca offsets as an expression of evolution

The analysis of the Boscolo-Galazzo et al. (2021) dataset performed here allows offsets through ancestor-descendent species to be tracked for the first time and the time of their appearance to be assessed. Specifically, we observe that offsets tend to appear with the origination of a new lineage and to continue to the modern representative(s) of that lineage (Fig. 8). In this way, an attempt can be made to interpret offsets as the geochemical expression of evolutionary new biochemical pathways or ecological strategies in emerging species.

For spinose species, the observed high Mg/Ca offset is shared by ancestor-descendent species such as *Globigerinella praesiphonifera–G. siphonifera* and *Praeorbulina glomerosa–Orbulina suturalis–O. universa* (Fig. 4). *Globigerina bulloides* shares the same type of offset as *Globigerinella* and a common ancestor (*Globigerina archaeobulloides*) in the earliest Oligocene (∼ 33.5 Ma) (Spezzaferri et al., 2018) (Fig. 4), suggesting that for this group the offset may go back to at least the early globigerinids of the Paleogene. The genus *Praeorbulina* originated from the genus *Trilobatus* at about 16 Ma (Fig. 4) (Pearson et al., 1997; Aze et al., 2011). *Trilobatus trilobus* is the last common ances-

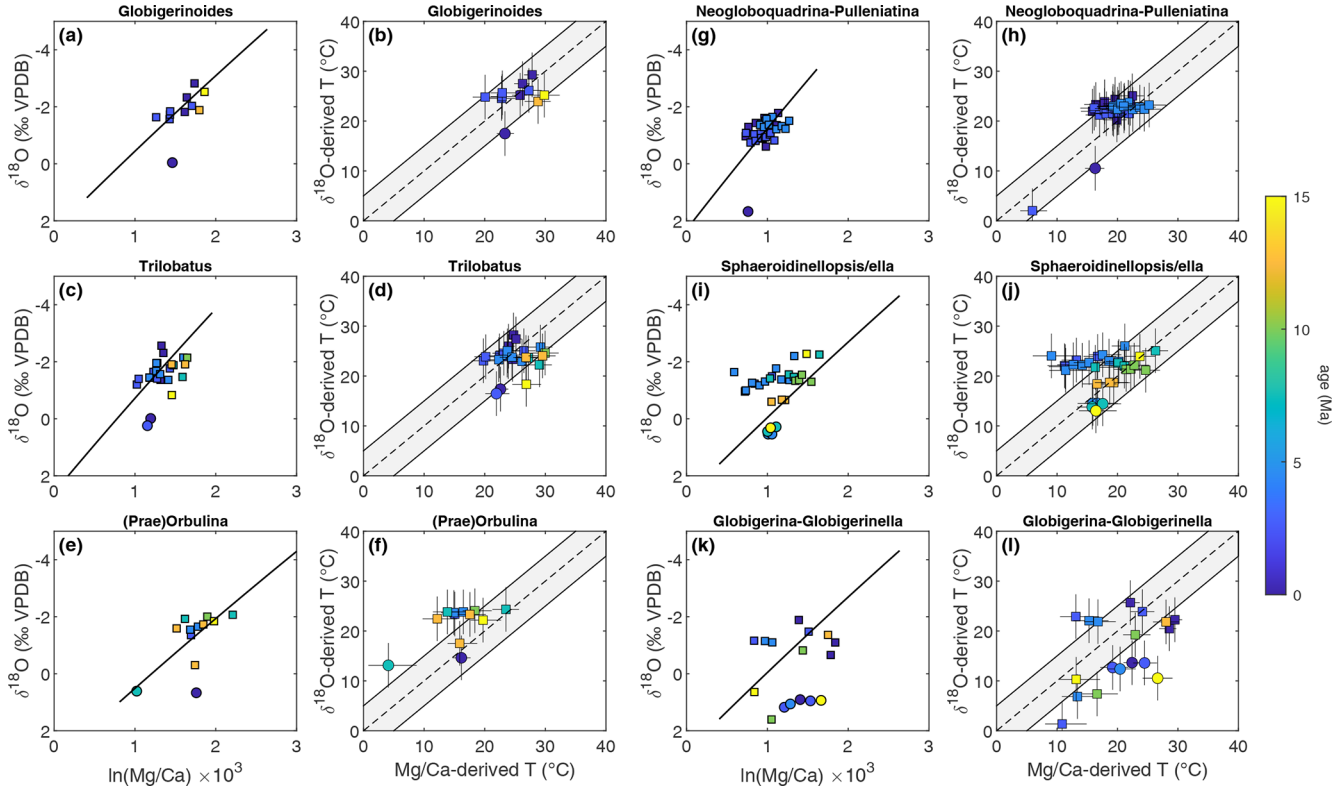

Figure 6. As in Fig. 5 extending the use of species-specific calibrations to all species in a lineage in the case of the *Trilobatus trilobus–T. sacculifer* **(c, d)**, *Praeorbulina glomerosa–Orbulina suturalis–O. universa* **(e, f)**, *Neogloboquadrina acostaensis–N. humerosa*, *N. pachyderma–N. incompta*, *N. acostaensis* and between related lineages in the case of *Neogloboquadrina* and the *Pulleniatina primalis–P. praecursor–P. finalis* lineage **(g, h)**. When applying species-specific calibrations, the offset between Mg/Ca and $\delta^{18}O$ temperature is resolved for some species (e.g. all *Neogloboquadrina*, compared to Fig. 5) but not for others; i.e. their reconstructed temperature still plots outside the grey error envelope (e.g. most of *Globigerina* and *Globigerinella*).

tor between the *Trilobatus* and *Praeorbulina–Orbulina* lineages (Fig. 4) and does not present offset Mg/Ca–$\delta^{18}O$ values, similar to its modern descendants (Figs. 4 and 5). This suggests that the offset in *Praeorbulina–Orbulina* originated within the lineage and the morphological changes associated with it (Fig. 8) and carried on to the modern representative *O. universa*. Spinose *Globigerinoides ruber* is also reported to be sensitive to pH changes (Kisakürek et al., 2008; Evans et al., 2016a), *G. ruber* is not offset in the analysed dataset (both in the raw data and calculated temperatures), with ancestor-descendent *G. subquadratus–G. ruber* behaving similarly to the *Trilobatus trilobus–T. sacculifer* lineage through time (Figs. 5 and 6), suggesting that this non-thermal effect is adequately accounted for in this case (Fig. 6) (i.e. the laboratory calibrations are applicable downcore into deep time in correcting for this). The Mg/Ca displayed by offset spinose *Praeorbulina–Orbulina*, *Globigerinella* species, and *G. bulloides* in the study dataset that is higher on average may suggest a lower pH environment, which we cannot directly account for (Fig. 2a). For *Globigerina* and *Globigerinella*, where a larger degree of scatter (Figs. 5 and 6k, l) is observed in association with a rather conservative morphology through time (Fig. 8), the offset may be linked to an opportunistic behaviour and capability to adapt to a broad range of environmental conditions with variable pH (Weiner et al., 2015). This may in turn be related to the complexity of genotypes association in both *G. bulloides* and *Globigerinella* species, with different genotypes having different ecologies but almost identical morphologies (e.g. Weiner et al., 2015; Morard et al., 2024).

We find that the low Mg/Ca offset is shared between ancestor-descendent lineages *Neogloboquadrina–Pulleniatina* and *Sphaeroidinellopsis–Sphaerodinella* (Figs. 4 and 8). *Neogloboquadrina* evolved from *Paragloborotalia continuosa* in the late Miocene, at about 10 Ma (Fig. 4). While paired Mg/Ca–$\delta^{18}O$ measurements for *P. continuosa* are not available, paired Mg/Ca–$\delta^{18}O$ measurements for *Paragloborotalia siakensis*, a species older than *P. continuosa*, do not show a low Mg/Ca offset (Table S1). This may indicate that the occurrence of low Mg/Ca crust/cortex started either with *P. continuosa*, the youngest representative of the genus *Paragloborotalia* in our study, or with the neogloboquadrinids. The genus *Pulleniatina* evolved from *Neogloboquadrina acostaensis* at about 6.5 Ma (Pearson

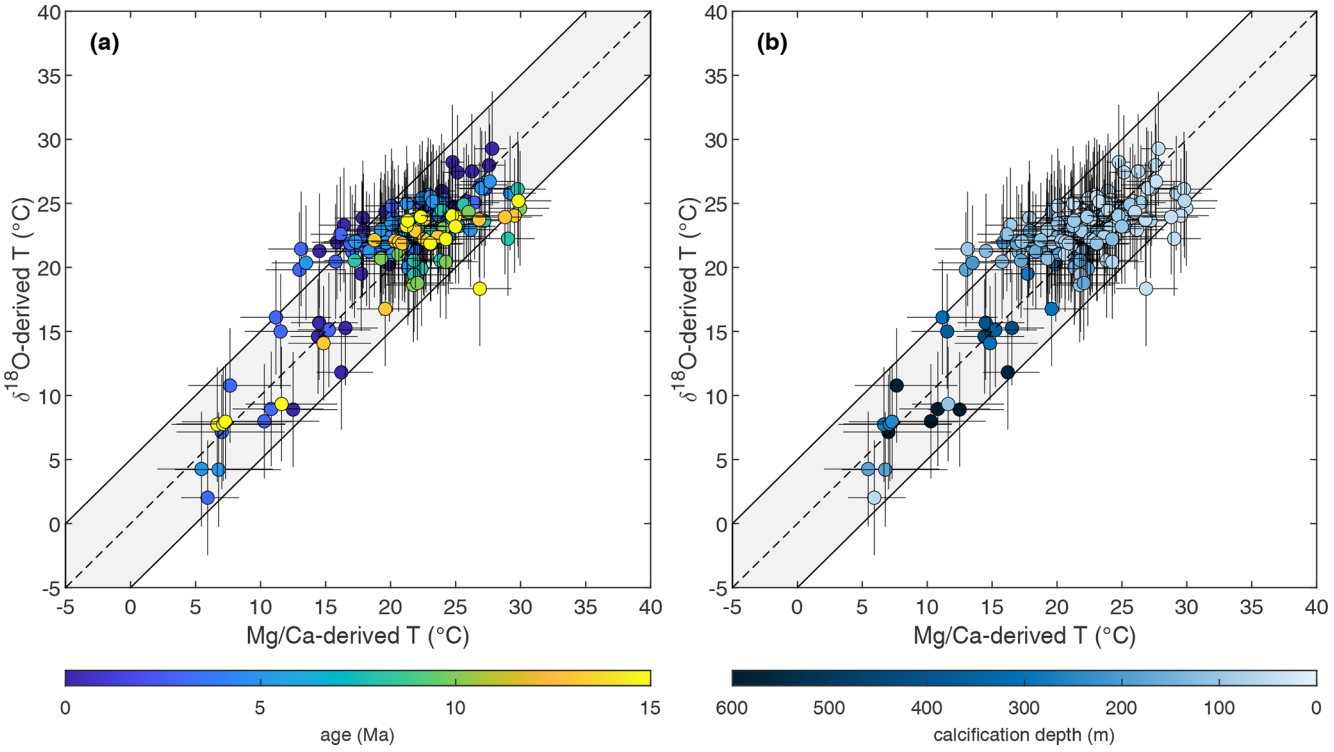

Figure 7. As Fig. 3, with all offset lineages (Sect. 4.3; specifically, those that remain offset following the application of lineage-specific calibrations where possible) and diagenetically compromised (Sect. 4.1) samples removed. Removing these samples leaves 157 data points, of which 92 % fall within the combined uncertainty of Mg/Ca–δ^{18}O agreement (grey envelope).

et al., 2023; see Fig. 4), by modifying the chambers' arrangement and progressively developing a cortex (Fig. 8). *Pulleniatina* may have inherited the capability to thicken its test from *Neogloboquadrina* and modified it into a cortex (Fig. 8) (Pearson et al., 2023). The occurrence of a low Mg/Ca cortex in *Pulleniatina* appears to start from the most ancient representative of this group, *P. primalis* (Fig. 4) and continues to the modern. Similar to *Paragloborotalia*, middle Miocene *Sphaeroidinellopsis kochi* and *S. seminulina* are not characterized by an offset to low Mg/Ca values (Figs. 4–6). Nonetheless, an offset is observed in 5 out of 10 specimens for late Miocene–early Pliocene *S. paenedehiscens* and always occurs for its descendant *Sphaeroidinella dehiscens* (Figs. 4–6). Our analysis shows how the occurrence of a low Mg/Ca offset in planktonic foraminifera becomes progressively rarer going back in time, in parallel with the rarity of crust/cortex features (Fig. 8). The occurrence of a crust/cortex is commonly observed in non-spinose modern planktonic foraminifera; however, only two early to middle Miocene genera are known to produce crusts (*Globoconella* and *Paragloborotalia*), and only one is known to produce a cortex (*Sphaeroidinellopsis*) (e.g. Fig. 8).

It is tempting to put the pattern of emergence of Mg/Ca offsets in relationship with changes in ocean chemistry and global climate over the last 15 Myr. In particular, the offset spinose species are mostly tropical and evolved during a time when mean ocean pH was more than 0.1 pH unit lower than the preindustrial period (Rae et al., 2021). Further, the *Praeorbulina–Orbulina* plexus evolved at about 16 Ma (Fig. 8), in coincidence with a drop in ocean pH, likely linked to the global warmth of the Miocene Climatic Optimum (Rae et al., 2021). The particularly high Mg/Ca signature of this group of species, along with their evolutionary timing, might testify their ability to withstand tropical surface waters more undersaturated than today thanks to changes in the biomineralization pathway as a consequence of their evolution during the Miocene Climatic Optimum.

The evolution of the offset non-spinose species happened several millions of years later during the long-term cooling trend of the last 10 Myr (Fig. 8). The offset species occur across tropical to high-latitude areas and mixed-layer (*Sphaeroidinellopsis*, *Sphaeroidinella*) to intermediate (*Neogloboquadrina*, *Pulleniatina*) depth habitats. The ability to develop a crust/cortex in species evolving over the last 10 Myr might have been of advantage as the global ocean was becoming progressively colder, in a similar way to the observed increases in shell mass across Pleistocene glacial cycles (e.g. Zarkogiannis et al., 2019).

The last 10 Myr was also characterized by decreasing concentration in Ca_{sw} ($[Ca^{2+}]$) in step with global cooling, reaching concentrations approximately half those of the middle Miocene in the Pleistocene (Zhou et al., 2021). Partly as a

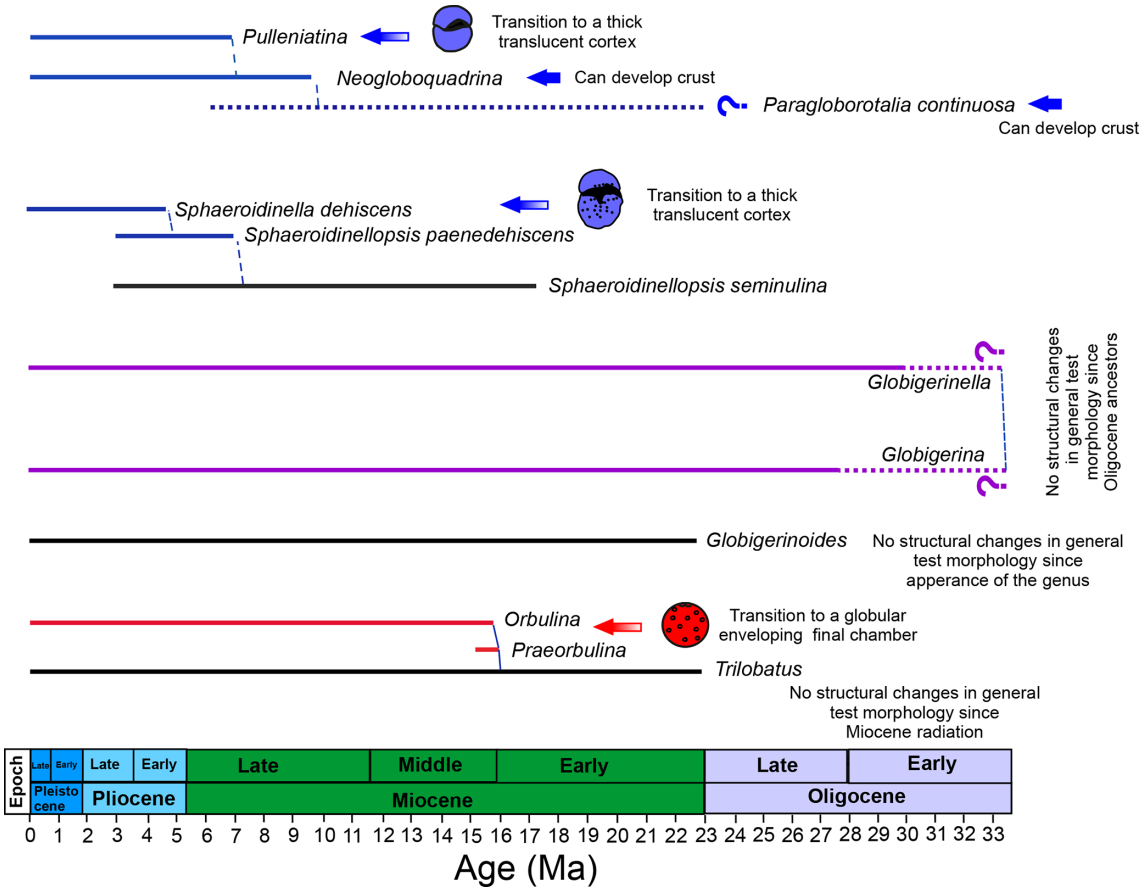

Figure 8. Simplified phylogeny for the offset lineages discussed in the text with the occurrence of morphological changes associated with their evolution highlighted. Coloured lines indicate species offset in Mg/Ca in the study dataset relative to a multispecies calibration approach, and black lines indicate non-offset species. Red lines indicate offset species with higher Mg/Ca, blue lines indicate offset species with lower Mg/Ca, and purple lines denote species displaying both types of offsets. Question marks indicate the lack of Mg/Ca data for a given species in the dataset presented here. Phylogeny after Aze et al. (2011) and Spezzaferri et al. (2018). The phylogenetic chart was generated using Mikrotax (Huber et al., 2016; http://www.mikrotax.org/pforams, last access: 4 June 2024). Ages are from Lourens et al. (2004) for the Neogene and Pälike et al. (2006) for the Oligocene.

consequence, Mg/Ca_{sw} approximately doubled over the past 15 Myr (Evans et al., 2016a; Rosenthal et al., 2022). With decreasing $[Ca^{2+}]$ and increasing $[Mg^{2+}]$ in seawater over the Neogene (Brennan et al., 2013; Evans et al., 2016a; Zhou et al., 2021), some species might have started to more actively control the Mg/Ca ratio at their biomineralization site, e.g. by proportionally increasing the active transport of Mg^{2+}, in order to buffer against the effects of the higher seawater Mg/Ca and to keep the outer parts of their shell with low Mg/Ca and thus more resistant to dissolution. Hence, the low Mg/Ca offset observed in the modern and fossil non-spinose species above might be linked to their evolutionary emergence during a time of changing ocean physical–chemical properties, which may have promoted the evolution of thicker tests with a different elemental chemistry making them less buoyant and resistant to dissolution.

5 Conclusions

We analysed a multispecies planktonic foraminiferal $\delta^{18}O$ and Mg/Ca dataset spanning the last 15 Myr from multiple locations to test whether temperature is the main controller of both proxies and assess the major overprinting factors through time and space and for species with very distinct ecologies. Once diagenesis and possible regional hydrographic factors are taken into account, we find that species-specific offsets not accounted for in our calibration strategy remain a source of mismatch between the two proxies. Specifically, *Globigerina*, *Globigerinella*, *Praeorbulina*, and *Orbulina* species are consistently offset, with Mg/Ca values higher than expected on average. Conversely, non-spinose *Neogloboquadrina*, *Pulleniatina*, *Sphaeroidinellopsis*, and *Sphaeroidinella* appear consistently offset with low Mg/Ca. The appearance of these geochemical offsets appears to be linked to the origination of new clades and is

shared between ancestor-descendent species, such that we were able to track their evolutionary history. The variable offset in *Globigerinella* may go back to the early globigerinids of the Paleogene and could be related to the opportunistic behaviour of this group and emergence of multiple genotypes through geological time, leading to a wider range of habitat conditions. The high Mg/Ca offset in *Orbulina* starts with *Praeorbulina* in the middle Miocene, while a low Mg/Ca offset appears typical of groups evolving in the late Neogene characterized by a crust or cortex. This pattern suggests that the offsets observed in modern species may be a legacy of their parent groups originating millions of years ago, when ocean properties were different from today.

Overall, our study highlights the power of the multispecies and multi-time slice dataset presented here, enabling us to identify the evolutionary origin and timing of deviations in Mg/Ca–temperature/pH relationships. Furthermore, our study demonstrates the robustness of Mg/Ca and $\delta^{18}O$ proxies through geologic time when nonthermal factors (especially Mg/Ca_{sw} and pH) are accounted for. For example, virtually all *Globigerinoides* and *Trilobatus* Mg/Ca- and $\delta^{18}O$-derived temperatures are within uncertainty of each other, highlighting the utility of these species for paleoceanographic reconstruction. In addition, our analysis enables us to identify species/lineages that should be treated with caution when interpreting Mg/Ca data, at the very least demonstrating that care should be taken in selecting the calibration approach and highlighting the need for further work in understanding the nonthermal controls on Mg incorporation into the shells of these foraminifera.

Code and data availability. All data are available in the Supplement of this paper. Code to perform the MgCaRB protocols is available on GitHub at https://github.com/dbjevans/MgCaRB/releases/tag/v1.3 (last access: 11 February 2025, https://doi.org/10.5281/zenodo.14056982, Evans, 2024) for MATLAB. The code to perform the calculations and produce the figures is available at https://doi.org/10.5281/zenodo.14847243 (Boscolo-Galazzo et al., 2025).

Supplement. The supplement related to this article is available online at https://doi.org/10.5194/bg-22-1095-2025-supplement.

Author contributions. EMM performed trace element analysis, FBG conceptualized the paper, DE performed data analysis, FBG and DE produced the figures, and FBG and DE wrote the paper with contributions from all authors.

Competing interests. The contact author has declared that none of the authors has any competing interests.

Disclaimer. Publisher's note: Copernicus Publications remains neutral with regard to jurisdictional claims made in the text, published maps, institutional affiliations, or any other geographical representation in this paper. While Copernicus Publications makes every effort to include appropriate place names, the final responsibility lies with the authors.

Acknowledgements. Samples for this study were provided by the International Ocean Discovery Program (IODP) and by the IODP, JOIDES Resolution, Expedition 363, West Pacific Warm Pool. We thank Lennart de Nooijer and an anonymous reviewer for constructive revisions. Marcin Latas assisted with sample preparation funded by an EU Marie-Curie Career Integration Grant 293741 to Bridget S. Wade. Flavia Boscolo-Galazzo acknowledges support from the EU Horizon 2020 Framework Programme (H2020-MSCA-IF-2020 101019438). Paul Minton is thanked for making Table S2.

Financial support. This research has been supported by the Natural Environment Research Council (NERC) grant NE/N001621/1 to Paul N. Pearson (Flavia Boscolo-Galazzo), NERC grant NE/P016375/1 to participate in IODP Expedition 363 (Paul N. Pearson), and NERC grant NE/N002598/1 to Bridget S. Wade (Elaine M. Mawbey), as well as the European Research Council, EU H2020 (grant nos. 293741 and 101019438).

The article processing charges for this open-access publication were covered by the University of Bremen.

Review statement. This paper was edited by Niels de Winter and reviewed by Lennart de Nooijer and one anonymous referee.

References

Anand, P., Elderfield, H., and Conte, M. H.: Calibration of Mg/Ca thermometry in planktonic foraminifera from a sediment trap time series, Paleoceanography, 18, 1050, https://doi.org/10.1029/2002PA000846, 2003.

Aze, T., Ezard, T. H. G., Purvis, A., Coxall, H. K., Stewart, D. R. M., Wade, B. S., and Pearson, P. N.: A phylogeny of Cenozoic macroperforate planktonic foraminifera from fossil data, Biol. Rev., 86, 900–927, https://doi.org/10.1111/j.1469-185X.2011.00178.x, 2011.

Barker, S., Greaves, M., and Elderfield, H.: A study of cleaning procedures used for foraminiferal Mg/Ca paleothermometry, Geochem. Geophy. Geosy., 4, 8407, https://doi.org/10.1029/2003GC000559, 2003.

Bemis, B. E., Spero, H. J., Bijma, J., and Lea, D. W.: Reevaluation of the oxygen isotopic composition of planktonic foraminifera: Experimental results and revised palaeotemperature equations, Paleoceanography, 13, 150–160, 1998.

Birch, H., Coxall, H. K., Pearson, P. N., Kroon, D., and O'Regan, M.: Planktonic foraminifera stable isotopes and water column structure: Disentangling eco-

logical signals, Mar. Micropaleontol., 10, 127–145, https://doi.org/10.1016/j.marmicro.2013.02.002, 2013.

Boscolo-Galazzo, F., Crichton, K. A., Ridgwell, A., Mawbey, E. M., Wade, B. S., and Pearson P. N.: Temperature controls carbon cycling and biological evolution in the ocean twilight zone, Science, 371, 1148–1152, https://doi.org/10.1126/science.abb6643, 2021.

Boscolo-Galazzo, F., Jones, A., Dunkley Jones, T., Crichton, K. A., Wade, B. S., and Pearson, P. N.: Late Neogene evolution of modern deep-dwelling plankton, Biogeosciences, 19, 743–762, https://doi.org/10.5194/bg-19-743-2022, 2022.

Boscolo-Galazzo, F., Evans, D., Mawbey, E. M., Gray, W. R., Pearson, P. N., and Wade, B. S.: Code and datasets to accompany Boscolo-Galazzo et al. (2025): Exploring macroevolutionary links in multi-species planktonic foraminiferal Mg / Ca and $\delta^{18}O$ from 15 Ma to Recent, Zenodo [code] and [data set], https://doi.org/10.5281/zenodo.14847243, 2025.

Branson, O., Read, E., Redfern, S. A. T., Rau, C., and Elderfield, H.: Revisiting diagenesis on the Ontong Java Plateau: Evidence for authigenic crust precipitation in *Globorotalia tumida*, Paleoceanography, 30, 1490–1502, https://doi.org/10.1002/2014PA002759, 2015.

Brennan, S. T., Lowenstein, T. K., and Cendon, D. I.: The major-ion composition of Cenozoic seawater: the past 36 million years from fluid inclusions in marine halite, Am. J. Sci., 313, 713–775, https://doi.org/10.2475/08.2013.01, 2013.

Chave, K. E.: Aspects of the biogeochemistry of magnesium 1. Calcareous marine organisms, J. Geol., 62, 266–283, https://doi.org/10.1086/626162, 1954.

Daëron, M. and Gray, W. R.: Revisiting oxygen-18 and clumped isotopes in planktic and benthic foraminifera, Paleoceanography and Paleoclimatology, 38, e2023PA004660, https://doi.org/10.1029/2023PA004660, 2023.

Davis, C. V., Fehrenbacher, J. S., Hill, T. M., Russell, A. D., and Spero, H. J.: Relationships between temperature, pH, and crusting on Mg/Ca ratios in laboratory-grown Neogloboquadrina foraminifera, Paleoceanography, 32, 2017PA003111, https://doi.org/10.1002/2017PA003111, 2017.

Dekens, P. S., Lea, D. W., Pak, D. K., and Spero, H. J.: Core top calibration of Mg/Ca in tropical foraminifera: Refining paleotemperature estimation, Geochem. Geophy. Geosy., 3, 1–29, https://doi.org/10.1029/2001GC000200, 2002.

Edgar, K. M., Anagnostou, E., Pearson, P. N., and Foster, G. L.: Assessing the impact of diagenesis on $\delta^{11}B$, $\delta^{13}C$, $\delta^{18}O$, Sr/Ca and B/Ca values in fossil planktic foraminiferal calcite, Geochim. Cosmochim. Ac., 166, 189–209, https://doi.org/10.1016/j.gca.2015.06.018, 2015.

Eggins S. M., Sadekov, A., and De Deckker P.: Modulation and daily banding of Mg/Ca in *Orbulina universa* tests by symbiont photosynthesis and respiration: a complication for seawater thermometry?, Earth Planet. Sc. Lett., 225, 411–419, https://doi.org/10.1016/j.epsl.2004.06.019, 2004.

Elderfield, H. and Ganssen, G.: Past temperature and $\delta^{18}O$ of surface ocean waters inferred from foraminiferal Mg / Ca ratios, Nature, 405, 442–445, 2000.

Emiliani, C.: Depth habitats of some species of pelagic foraminifera as indicated by oxygen isotope ratios, Am. J. Sci., 252, 149–158, 1954.

Erez, J. and Luz, B.: Experimental paleotemperature equation for planktonic foraminifera, Geochim. Cosmochim. Ac., 47, 1025–1031, https://doi.org/10.1016/0016-7037(83)90232-6, 1983.

Evans, D.: dbjevans/MgCaRB: v1.3 (v1.3), Zenodo [code], https://doi.org/10.5281/zenodo.14056982, 2024.

Evans D., Erez J., Oron S., and Muller W.: Mg/Ca temperature and seawater-test chemistry relationships in the shallow-dwelling large benthic foraminifera *Operculina ammonoides*, Geochim. Cosmochim. Ac., 148, 325–342, https://doi.org/10.1016/j.gca.2014.09.039, 2015.

Evans, D., Brierley, C., Raymo, M. E., Erez, J., and Müller, W.: Planktic foraminifera shell chemistry response to seawater chemistry: Pliocene–Pleistocene seawater Mg/Ca, temperature and sea level change, Earth Planet. Sc. Lett., 438, 139–148, https://doi.org/10.1016/j.epsl.2016.01.013, 2016a.

Evans, D., Wade, B. S., Henehan, M., Erez, J., and Müller, W.: Revisiting carbonate chemistry controls on planktic foraminifera Mg/Ca: implications for sea surface temperature and hydrology shifts over the Paleocene–Eocene Thermal Maximum and Eocene–Oligocene transition, Clim. Past, 12, 819–835, https://doi.org/10.5194/cp-12-819-2016, 2016b.

Fabbrini, A., Zaminga, I., Ezard, T., and Wade, B. S.: Systematic taxonomy of middle Miocene *Sphaeroidinellopsis* (planktonic foraminifera), J. Syst. Palaeontol., 19, 953–968, https://doi.org/10.1080/14772019.2021.1991500, 2021.

Fayolle, F. and Wade, B. S.: Data report: Miocene planktonic foraminifers *Dentoglobigerina* and *Globoquadrina* from IODP Sites U1489 and U1490, Expedition 363, in: Western Pacific Warm Pool. Proceedings of the International Ocean Discovery Program, edited by: Rosenthal, Y., Holbourn, A. E., Kulhanek, D. K., and the Expedition 363 Scientists, 363, College Station, TX (International Ocean Discovery Program), https://doi.org/10.14379/iodp.proc.363.203.2020, 2020.

Fehrenbacher, J. S. and Martin, P. A.: Exploring the dissolution effect on the intrashell Mg / Ca variability of the planktic foraminifer Globigerinoides ruber, Paleoceanography, 29, 854–868, 2014.

Friedrich, O., Schiebel, R., Wilson, P. A., Weldeab, S., Beer, C. J., Cooper, M. J., and Fiebig, J.: Influence of test size, water depth, and ecology on Mg/Ca, Sr/Ca, $\delta^{18}O$ and $\delta^{13}C$ in nine modern species of planktic foraminifers, Earth Planet. Sc. Lett., 319, 133–145, https://doi.org/10.1016/j.epsl.2011.12.002, 2012.

Fritz-Endres, T. and Fehrenbacher, J.: Preferential loss of high trace element bearing inner calcite in foraminifera during physical and chemical cleaning, Geochem. Geophy. Geosy., 22, e2020GC009419, https://doi.org/10.1029/2020GC009419, 2021.

Gaskell, D. E. and Hull, P. M.: Technical note: A new online tool for $\delta^{18}O$-temperature conversions, Clim. Past, 19, 1265–1274, https://doi.org/10.5194/cp-19-1265-2023, 2023.

Gaskell, D. E., Huber, M., O'Brien, C. L., Inglis, G. N., Acosta, R. P., Poulsen, C. J., and Hull, P. M.: The latitudinal temperature gradient and its climate dependence as inferred from foraminiferal ^{18}O over the past 95 million years, P. Natl. Acad. Sci. USA, 119, e2111332119, https://doi.org/10.1073/pnas.2111332119, 2022.

Gray, W. R. and Evans, D.: Nonthermal influences on Mg/Ca in planktonic foraminifera: A review of culture studies and application to the last glacial maximum, Paleoceanography and Paleocli-

matology, 34, 306–315, https://doi.org/10.1029/2018PA003517, 2019.

Gray, W. R., Weldeab, S., Lea, D. W., Rosenthal, Y., Gruber, N., Donner, B., and Fischer, G.: The effects of temperature, salinity, and the carbonate system on Mg/Ca in *Globigerinoides ruber* (white): A global sediment trap calibration, Earth Planet. Sc. Lett., 482, 607–620, https://doi.org/10.1016/j.epsl.2017.11.026, 2018.

Holland, K., Branson, O., Haynes, L. L., Honisch, B., Allen, K. A., Russell, A. D., Fehrenbacher, J. S., Spero, H. J., and Eggins S. M.: Constraining multiple controls on planktic foraminifera Mg/Ca, Geochim. Cosmochim. Ac., 273, 116–136, https://doi.org/10.1016/j.gca.2020.01.015, 2020.

Hönisch, B., Allen, K. A., Lea, D. W., Spero, H. J., Eggins, S. M., Arbuszewski, J., deMenocal, P., Rosenthal, Y., Russell, A. D., and Elderfield, H.: The influence of salinity on Mg/Ca in planktic foraminifers – evidence from cultures, core-top sediments and complementary $\delta^{18}O$, Geochim. Cosmochim. Acta, 121, 196–213, https://doi.org/10.1016/j.gca.2013.07.028, 2013.

Huber, B. T., Petrizzo, M. R., Young, J., Falzoni, F., Gilardoni, S., Bown, P. R., and Wade, B. S.: Pforams@mikrotax: A new online taxonomic database for planktonic foraminifera, Micropalaeontology, 62, 429–438, 2016.

John, E. H., Staudigel, P. T., Buse, B., Lear, C. H., Pearson, P. N., and Slater, S. M.: Revealing their true stripes: Mg/Ca banding in the Paleogene planktonic foraminifera genus *Morozovella* and implications for paleothermometry, Paleoceanography and Paleoclimatology, 38, e2023PA004652, https://doi.org/10.1029/2023PA004652, 2023.

Jonkers, L., de Nooijer, L. J., Reichart, G.-J., Zahn, R., and Brummer, G.-J. A.: Encrustation and trace element composition of *Neogloboquadrina dutertrei* assessed from single chamber analyses – implications for paleotemperature estimates, Biogeosciences, 9, 4851–4860, https://doi.org/10.5194/bg-9-4851-2012, 2012.

Jonkers, L., Gopalakrishnan, A., Weßel, L., Chiessi, C. M., Groeneveld, J., Monien, P., Douglas, L., and Morard, R.: Morphotype and crust effects on the geochemistry of *Globorotalia inflata*, Paleoceanography and Paleoclimatology, 36, e2021PA004224, https://doi.org/10.1029/2021PA004224, 2021.

Katz, M. E., Miller, K. G., Wright, J. D., Wade, B. S., Browning, J. V., Cramer, B. S., and Rosenthal, Y.: Stepwise transition from the Eocene greenhouse to the Oligocene icehouse, Nat. Geosci., 1, 329–334, 2008.

Kim, S.-T., and O'Neil, J. R.: Equilibrium and non-equilibrium oxygen isotope effects in synthetic carbonates, Geochim. Cosmochim. Ac., 61, 3461–3475, 1997.

Kısakürek, B., Eisenhauer, A., Böhm, F., Garbe-Schönberg, D., and Erez, J.: Controls on shell Mg/Ca and Sr/Ca in cultured planktonic foraminiferan, *Globigerinoides ruber* (white), Earth Planet. Sc. Lett., 273, 260–269, https://doi.org/10.1016/j.epsl.2008.06.026, 2008.

LeGrande A. N. and Schmidt G. A.: Global gridded data set of the oxygen isotopic composition in seawater, Geophys. Res. Lett., 33, L12604, https://doi.org/10.1029/2006GL026011, 2006.

Lea, D. W., Mashiotta, T. A., and Spero, H. J.: Controls on magnesium and strontium uptake in planktonic foraminifera determined by live culturing, Geochim. Cosmochim. Ac., 63, 2369–2379, https://doi.org/10.1016/S0016-7037(99)00197-0, 1999.

Lear, C. H., Elderfield, H., and Wilson, P. A.: Cenozoic deep-sea temperatures and global ice volumes from Mg / Ca in benthic foraminiferal calcite, Science, 287, 269–272, 2000.

Lear, C. H., Rosenthal, Y., and Slowey, N.: Benthic foraminiferal Mg/Ca-paleothermometry: A revised core-top calibration, Geochim. Cosmochim. Ac., 66, 3375–3387, https://doi.org/10.1016/S0016-7037(02)00941-9, 2002.

Leckie, R. M., Wade, B. S., Pearson, P. N., Fraass, A. J., King, D. J., Olsson, R. K., Premoli Silva, I., Spezzaferri, S., and Berggren, W. A.: Taxonomy, biostratigraphy, and phylogeny of Oligocene and early Miocene *Paragloborotalia* and *Parasubbotina*, in: Atlas of Oligocene Planktonic Foraminifera, edited by: Wade, B. S., Olsson, R. K., Pearson, P. N., Huber, B. T., and Berggren, W. A., Cushman Foundation of Foraminiferal Research, Special Publication, 46, 125–178, ISBN 9781970168419, 2018.

Locarnini, R. A., Mishonov, A. V., Antonov, J. I., Boyer, T. P., Garcia, H. E., Baranova, O. K., Zweng, M. M., Paver, C. R., Reagan, J. R., Johnson, D. R., Hamilton, M., and Seidov, D.: World Ocean Atlas 2013, Volume 1: Temperature, edited by: Levitus, S., Mishonov, A., NOAA Atlas NESDIS 73, 40 pp., https://doi.org/10.7289/V55X26VD, 2013.

Lourens, L. J., Hilgen, F. J., Shackleton, N. J., Laskar, J., and Wilson, D.: The Neogene Period, in: Geological Time Scale 2004, edited by: Gradstein, F. M., Ogg, J. G., and Smith, A. G., Cambridge University Press, 409–440, https://doi.org/10.1016/B978-0-12-824360-2.00029-2, 2004.

Malevich, S. B., Vetter, L., and Tierney, J. E.: Global Core Top Calibration of ^{18}O in Planktic Foraminifera to Sea Surface Temperature, Paleoceanography and Paleoclimatology, 34, 1292–1315, https://doi.org/10.1029/2019PA003576, 2019.

Mathien-Blard, E. and Bassinot, F.: Salinity bias on the foraminifera Mg/Ca thermometry: correction procedure and implications for past ocean hydrographic reconstructions, Geochem. Geophys. Geosyst., 10, Q12011, https://doi.org/10.1029/2008GC002353, 2009.

McConnell, M. C. and Thunell, R. C.: Calibration of the planktonic foraminiferal Mg/Ca paleothermometer: sediment trap results from the Guaymas Basin, Gulf of California, Paleoceanography, 20, PA2016, https://doi.org/10.1029/2004PA001077, 2005.

Miller, K. G., Browning, J. V., Schmelz, W. J., Kopp, R. E., Mountain, G. S., and Wright, J. D.: Cenozoic sea-level and cryospheric evolution from deep-sea geochemical and continental margin records, Science Advances, 6, eaaz1346, https://doi.org/10.1126/sciadv.aaz1346, 2020.

Morard, R., Darling, K. F., Weiner, A. K. M., Hassenrück, C., Vanni, C., Cordier, T., Henry, N., Greco, M., Vollma, N. M., Milivojevic, T., Rahman, S. N., Siccha, M., Meilland, J., Jonkers, L., Quillévéré, F., Escarguel, G., Douady, C. J., de Garidel-Thoron, T., de Vargas, C., and Kucera, M.: The global genetic diversity of planktonic foraminifera reveals the structure of cryptic speciation in plankton, Biol. Rev., 99, 1218–1241, https://doi.org/10.1111/brv.13065, 2024.

Mohtadi, M., Steinke, S., Groeneveld, J., Fink, H. G., Rixen, T., Hebbeln, D., Donner, B., and Herunadi, B.: Low-latitudecontrol on seasonal and interannual changes in planktonic foraminiferal flux and shell geochemistry off south Java: A sediment trapstudy, Paleoceanography, 24, PA1201, https://doi.org/10.1029/2008PA001636, 2009.

Mucci, A.: Influence of temperature on the composition of magnesian calcite overgrowths precipitated from seawater, Geochim. Cosmochim. Ac., 51, 1977–1984, https://doi.org/10.1016/0016-7037(87)90186-4, 1987.

Mucci, A. and Morse, J. W.: The incorporation of Mg^{2+} and Sr^{2+} into calcite overgrowths: influences of growth rate and solution composition, Geochim. Cosmochim. Ac., 47, 217–233, https://doi.org/10.1016/0016-7037(83)90135-7, 1983.

Nuernberg, D.: Magnesium in tests of *Neogloboquadrina pachyderma* sinistral from high northern and southern latitudes, J. Foramin. Res., 25, 350–368, https://doi.org/10.2113/gsjfr.25.4.350, 1995.

Nürnberg, D., Bijma, J., and Hemleben, C.: Assessing the reliability of magnesium in foraminiferal calcite as a proxy for water mass temperatures, Geochim. Cosmochim. Ac., 60, 803–814, https://doi.org/10.1016/0016-7037(95)00446-7, 1996.

Opdyke, B. N. and Pearson, P. N.: Data report: geochemical analysis of multiple planktonic foraminifer species at discrete time intervals, in: Proceedings of the Ocean Drilling Program, Scientific Results, 144, edited by: Haggerty, J. A., Premoli Silva, I., Rack, F., and McNutt, M. K., 993–995, https://doi.org/10.2973/odp.proc.sr.144.052.1995, 1995.

Pälike, H., Norris, R. D., Herrle, J. O., Wilson, P. A., Coxall, H. K., Lear, C. H., Shackleton, N. J., Tripati, A. K., and Wade, B. S.: The heartbeat of the Oligocene climate system, Science, 314, 1894–1898, https://doi.org/10.1126/science.1133822, 2006.

Pearson, P. N., Shackleton, N. J., and Hall, M. A.: Stable isotopic evidence for the sympatric divergence of *Globigerinoides trilobus* and *Orbulina universa*, J. Geol. Soc. London, 154, 295–302, https://doi.org/10.1144/gsjgs.154.2.0295, 1997.

Pearson, P. N.: Oxygen isotopes in foraminifera: overview and historical review, in: Reconstructing Earth's Deep-Time Climate, Paleontological Society Papers, vol. 18, edited by: Ivany, L. and Huber, B., 1–38, Cambridge University Press, https://doi.org/10.1017/S1089332600002539, 2012.

Pearson, P. N., Young, J., King, D. J., and Wade, B. S.: Biochronology and evolution of *Pulleniatina* (planktonic foraminifera), J. Micropalaeontol., 42, 211–255, https://doi.org/10.5194/jm-42-211-2023, 2023.

Rae, J. W. B., Zhang, Y., Liu, X., Foster, G. L., Stoll, H. M., and Whiteford, D. M.: Atmospheric CO_2 over the past 66 million years from marine archives, Annu. Rev. Earth Pl. Sc., 49, 609–641, https://doi.org/10.1146/annurev-earth-082420-063026, 2021.

Regenberg, M., Steph, S., Nürnberg, D., Tiedemann, R., and Garbe-Schönberg, D.: Calibrating Mg / Ca ratios of multiple planktonic foraminiferal species with $\delta^{18}O$-calcification temperatures: Paleothermometry for the upper water column, Earth Planet. Sc. Lett., 278, 324–336, 2009.

Regenberg, M., Regenberg, A., Garbe-Schönberg, D., and Lea, D. W.: Global dissolution effects on planktonic foraminiferal Mg/Ca ratios controlled by the calcite-saturation state of bottom waters, Paleoceanography, 29, 127–142, https://doi.org/10.1002/2013PA002492, 2014.

Rohling, E. J., Foster, G. L., Gernon, T. M., Grant, K. M., Heslop, D., Hibbert, F. D., Roberts, A. P., and Yu, J.: Comparison and synthesis of sea-level and deep-sea temperature variations over the past 40 million years, Rev. Geophys., 60, e2022RG000775, https://doi.org/10.1029/2022RG000775, 2022.

Rongstad, B. L., Marchitto, T. M., and Herguera, J. C.: Understanding the effects of dissolution on the Mg/Ca paleothermometer in planktic foraminifera: Evidence from a novel individual foraminifera method, Paleoceanography, 32, 1386–1402, https://doi.org/10.1002/2017PA003179, 2017.

Rosenthal, Y., Bova, S., and Zhou, X.: A user guide for choosing planktic foraminiferal Mg/Ca-temperature calibrations. Paleoceanography and Paleoclimatology, 37, e2022PA004413, https://doi.org/10.1029/2022PA004413, 2022.

Russell, A. D., Honisch, B., Spero, H. J., and Lea, D. W.: Effects of seawater carbonate ion concentration and temperature on shell U, Mg, and Sr in cultured planktonic foraminifera, Geochim. Cosmochim. Ac., 68, 4347–4361, https://doi.org/10.1016/j.gca.2004.03.013, 2004.

Sexton, P. E., Wilson, P. A., and Pearson, P. N.: Microstructural and geochemical perspectives on planktic foraminiferal preservation: "Glassy" versus "Frosty", Geochem. Geophy. Geosy., 7, Q12P19, https://doi.org/10.1029/2006GC001291, 2006.

Schiebel, R. and Hemleben, C.: Planktic foraminifers in the modern ocean, Springer, 366 pp., ISBN 978-3-662-50295-2, https://doi.org/10.1007/978-3-662-50297-6, 2017.

Spero, H. J., Bijma, J., Lea, D. W., and Bemis, B. E.: Effect of seawater carbonate concentration on foraminiferal carbon and oxygen isotopes, Nature, 390, 497–500, https://doi.org/10.1038/37333, 1997.

Spezzaferri, S., Coxall, H. K., Olsson, R. K., and Hemleben, C.: Taxonomy, biostratigraphy and phylogeny of Oligocene *Globigerina*, *Globigerinella*, and *Quiltyella* n. gen., in: Atlas of Oligocene Planktonic Foraminifera, Cushman Foundation of Foraminiferal Research, edited by: Wade, B. S., Olsson, R. K., Pearson, P. N., Huber, B. T., and Berggren, W. A., Special Publication, Cushman Foundation for Foraminiferal research, 46, 125–178, 2018.

Spratt, R. M. and Lisiecki, L. E.: A Late Pleistocene sea level stack, Clim. Past, 12, 1079–1092, https://doi.org/10.5194/cp-12-1079-2016, 2016.

Staudigel, P. T., John, E. H., Buse, B., Pearson, P. N., and Lear, C. H.: Apparent preservation of primary foraminiferal Mg/Ca ratios and Mg-banding in recrystallized foraminifera, Geology, 50, 760–764, https://doi.org/10.1130/G49984.1, 2022.

Tierney, J. E., Malevich, S. B., Gray, W., Vetter, L., and Thirumalai, K.: Bayesian calibration of the Mg/Ca paleothermometer in planktic foraminifera, Paleoceanography and Paleoclimatology, 34, 2005–2030, https://doi.org/10.1029/2019PA003744, 2019.

Urey, H. C.: The thermodynamic properties of isotopic substance, J. Chem. Soc., 1947, 562–581, 1947.

Von Langen, P. J., Pak, D. K., Spero, H. J., and Lea, D. W.: Effects of temperature on Mg/Ca in neogloboquadrinid shells determined by live culturing, Geochem. Geophy. Geosy., 6, Q10P03, https://doi.org/10.1029/2005GC000989, 2005.

Wade, B. S., Pearson, P. N., Berggren, W. A., and Pälike, H.: Review and revision of Cenozoic tropical planktonic foraminiferal biostratigraphy and calibration to the geomagnetic polarity and astronomical time scale, Earth-Sci. Rev., 104, 111–142, https://doi.org/10.1016/j.earscirev.2010.09.003, 2011.

Weiner, A. K. M., Weinkauf, M. F. G., Kurasawa, A., Darling, K. F., and Kucera, M.: Genetic and morphometric evidence for parallel evolution of the *Globiger-*

inella calida morphotype, Mar. Micropaleontol., 114, 19–35, https://doi.org/10.1016/j.marmicro.2014.10.003, 2015.

Westerhold, T., Marwan, N., Drury, A. J., Liebrand, D., Agnini, C., Anagnostou, E., Barnet, J. S. K., Bohaty, S. M., Vleeschouwer, D. D., Florindo, F., Frederichs, T., Hodell, D. A., Holbourn, A. E., Kroon, D., Lauretano, V., Littler, K., Lourens, L. J., Lyle, M., Pälike, H., Röhl, U., Tian, J., Wilkens, R. H., Wilson, P. A., and Zachos, J. C.: Anastronomically dated record of Earth's climate and its predictability over the last 66 million years, Science, 369, 1383–1387, https://doi.org/10.1126/science.aba6853, 2020.

Yu, J., Elderfield, H., Greaves, M., and Day, J.: Preferential dissolution of benthic foraminiferal calcite during laboratory reductive cleaning, Geochem. Geophy. Geosy., 8, Q06016, https://doi.org/10.1029/2006GC001571, 2007.

Zarkogiannis, S. D., Antonarakou, A., Tripati, A., Kontakiotis, G., Mortyn, P. G., Drinia, H., and Greaves, M.: Influence of surface ocean density on planktonic foraminifera calcification, Sci. Rep.-UK, 9, 533, https://doi.org/10.1038/s41598-018-36935-7, 2019.

Zeebe, R. E.: An explanation of the effect of sea water carbonate concentration on foraminiferal oxygen isotopes, Geochim. Cosmochim. Ac., 63, 2001–2007, https://doi.org/10.1016/S0016-7037(99)00091-5, 1999.

Zeebe, R. E. and Tyrrell, T.: History of carbonate ion concentration over the last 100 million years II: revised calculations and new data, Geochim. Cosmochim. Ac., 257, 373–392, https://doi.org/10.1016/j.gca.2019.02.041, 2019.

Zhou, X., Rosenthal, Y., Haynes, L., Si W., Evans, D., Huang, K.-F., Honisch, B., and Erez, J.: Planktic foraminiferal Na/Ca: A potential proxy for seawater calcium concentration, Geochim. Cosmochim. Ac., 305, 306–322, https://doi.org/10.1016/j.gca.2021.04.012, 2021.